Journal of Biological Systems, Vol. 23, No. 1 (2015) 131–163

DOI: 10.1142/S0218339015500084

World Scientific
www.worldscientific.com

A MATHEMATICAL MODEL TO ASSESS THE IMMUNE RESPONSE AGAINST *TRYPANOSOMA CRUZI* INFECTION

HYUN MO YANG
UNICAMP – IMECC – DMA
Praça Sérgio Buarque de Holanda, 651
CEP: 13083-859, Campinas, SP, Brazil
hyunyang@ime.unicamp.br

Received 14 August 2014
Revised 21 October 2014
Accepted 29 October 2014
Published 21 January 2015

A mathematical model is developed to assess humoral and cellular immune responses against *Trypanosoma cruzi* infection. Analysis of the model shows a unique non-trivial equilibrium, which is locally asymptotically stable, except in the case of a strong cellular response. When the proliferation of the activated CD8 T cells is increased, this equilibrium becomes unstable and a limit cycle appears. However, this behavior can be avoided by increasing the action of the humoral response. Therefore, unbalanced humoral and cellular responses can be responsible for long asymptomatic period, and the control of *Trypanosoma cruzi* infection is a consequence of well coordinated action of both humoral and cellular responses.

Keywords: Chagas' Disease; Humoral and Cellular Immune Responses; Deterministic Model; Limit Cycle.

1. Introduction

Trypanosoma cruzi, the causative agent of American trypanosomiasis (or Chagas' disease), is transmitted by various species of bloodsucking triatomine insects, or kissing bugs. Other forms of transmission include consumption of uncooked food contaminated with feces from infected bugs, congenital transmission, blood transfusion, organ transplantation and accidental laboratory exposure. *T. cruzi* infection is a zoonosis, and humans are merely unfortunate hosts whose involvement in the cycle of transmission is not necessary for the perpetuation of the parasite in nature. It is currently estimated by the Pan American Health Organization that 10 to 12 million people are infected with *T. cruzi* and that up to 45,000 persons die each year of Chagas' disease.[1]

The insects become infected by sucking blood from animals or humans that have circulating trypomastigotes. The injected parasites multiply in the midgut of the insects as epimastigotes, which are flagellates of a distinct morphological

type, and in the hindgut transform into infective metacyclic trypomastigotes that are discharged with the feces at the time of subsequent blood meal. Transmission to humans occurs when mucous membranes, conjunctivae or breaks in the skins are contaminated with bug feces containing the infective form. In humans, American trypanosomes enter a variety of host cell types and multiply in the cytoplasm after transformation into amastigotes. When multiplying amastigotes fill the host cell, they differentiate into trypomastigotes in about 24 h, and the cell ruptures. The time from trypomastigote penetration of a cell to its rupture is thought to be about five days, but it varies according to cell size and strain differences. The released parasites invade local tissues or spread hematogenously to distinct sites, this initiating further cycles of multiplication, primarily in muscle cells, and maintaining a parasitemia infective for vectors. In contrast, African trypanosomes, which cause sleeping sickness in humans, do not have an intracellular form and multiply as trypomastigotes that circulate in the mammalian blood stream and other extracellular spaces.[1]

Mathematical models for Chagas' disease transmission among humans and sylvatic transmission were presented by Inaba and Sakine[2] and Kribs-Zaleta,[3] respectively, while Cohen and Gürtler[4] considered household transmission. Kleinman and Busch[5] modeled the risk of transfusion-transmitted infection; and Slimi *et al.*[6] applied cellular automata formalism to describe the spatial spread of Chagas disease. In many countries, such as Brazil, *T. cruzi* infection by insects was eradicated, but new cases of infection can occur due to congenital transmission.[7]

Within humans, the immune response against *T. cruzi* eliminates or contains the infection. In experimental models, both CD4 and CD8 T cells have been shown to be important for resistance to *T. cruzi*. Lysis of infected macrophages by CD8-positive, cytotoxic T cells may also be an important mechanism of host defense. CD4 T cells are also necessary to generate the specific antibody that contributes to parasite clearance. Both types of T cells produce cytokines, principally interferon gamma (IFN-γ), capable of activating macrophages to kill intracellular amastigotes. However, the pathogenicity of experimental *T. cruzi* infections has been linked to the induction of immunosuppressive cytokines by the parasite following infection, which inhibit the macrophage activation capability of IFN-γ.[8]

It is logical that an organism so well adapted for intracellular survival should have the ability to increase macrophage cytokines that prevent its destruction. Circulating trypomastigotes shed a glycoprotein that inhibits the formation of complement C3 converterases and accelerates their decay, which avoid the immune response and persist for years in host. However, host antibodies are eventually generated that neutralize this protective glycoprotein, exposing the trypomastigotes to complement-mediated lysis. These antibodies play an important role in the suppression of circulating trypomastigotes in patients with chronic disease. After entering the circulation, trypomastigotes must identify and infect susceptible host cells. The penetration of trypanosomes into a variety of host cell types

probably occurs through receptor–ligand-mediated endocytosis (macrophages and monocytes, as well as trypomastigotes, have fibronectin receptors, a molecule that enhances both parasite-cell binding and parasite uptake). As intracellular parasites, they must evade intracellular killing mechanisms, and a proportion of trypomastigotes pass through the phagosomal membrane to infect the cytoplasm, a privileged site free from lysosomal enzymes.[8]

Therefore, both humoral and cellular responses promoted by the action of CD4 T cells in order to subdue *T. cruzi* infection are essential. The aim of this paper is the development of a mathematical model to assess the role played by humoral and cellular immune responses to control *T. cruzi* infection. Isasi *et al.*[9] and Sibona *et al.*[10] analyzed mathematical models taking into account the parasite population and the diversity of antibodies, while Velasco–Hernandez and Perez–Chavela analyzed a model for the cellular immune response to *T. cruzi*.[11]

The paper is structured as follows. In Sec. 2, a simple mathematical model of the immune system responding to *T. cruzi* infection is developed, and the analysis of the model is presented. In Secs. 3 and 4, numerical results are obtained to assess the immune responses, and discussions regarding the appearance of a limit cycle and parasitemia are presented. Conclusions are presented in Sec. 5.

2. Model

In the model, all cells potentially involved in the immune response are not included, such as CD4 T cells, dendritic cells, macrophages, NK cells, eosinophils, etc. A simple model presented here does not consider the production of cytokines that down- and up-regulate the immune response. Instead, it is assumed that the activation and proliferation of immune response cells are simply proportional to the amount of parasites.

Trypanosomes (denoted by T, the concentration of trypanosomes circulating in the blood stream at time t) infect susceptible host cells (denoted by H), resulting in infected cells (denoted by I). Inside the cell, trypomastigotes transform into amastigotes, and they multiply. When amastigotes fill the host cell, they differentiate into trypomastigotes, which are released after the cell ruptures. To clear the circulating parasites and infected cells, both naive B (denoted by B) and CD8 T (denoted by C) cells must be activated by activated CD4 T cells. Here, activation of naive cells is assumed to be mediated by the circulating parasites as well as their proliferation. The concentrations at time t of activated B and CD8 T cells are denoted, respectively, by B_a (plasma cells) and Ca (cytotoxic cells). Finally, the occurrence of infection, and activation and proliferation of immune cells follow the mass action law.

With respect to the blood stream circulating *T. cruzi*: (1) the parasites are under a natural mortality rate μ_T; (2) an average number n of parasites can penetrate a susceptible host cell at a constant infection rate α and (3) they are killed by

direct and indirect actions of antibodies excreted by plasma cells at a constant humoral response rate ε. Susceptible host cells are under natural mortality rate μ_H, and they are replenished at a constant rate λ_H. Infected cells are either led to death and release huge number of *T. cruzi*, or killed by cytotoxic cells at a constant cellular response rate β. Hence, infected cells are under additional mortality μ_I, besides the natural mortality rate μ_H, and each cell releases on average τ parasites. Naive immune system cells are replenished at constant rates λ_B and λ_C, and are under natural mortality rates μ_B and μ_C. They can also be activated at constant rates γ_B and γ_C. With respect to the activated cells, the proliferation rates are given by δ_B and δ_C and the additional mortality rates are μ_B^d and μ_C^d, which are due to the intense proliferation and production of immune components. After the clearance of parasites by the immune system, activated cells must be eliminated by apoptosis.

Based on the above definitions of variables and parameters of the model, the dynamics of the interaction between immune system and *T. cruzi* infection is described by the following system of equations

$$\begin{cases} \dfrac{d}{dt}T = \tau(\mu_H + \mu_I)I - \mu_T T - n\alpha TH - \varepsilon B_a T, \\ \dfrac{d}{dt}H = \lambda_H - \mu_H H - \alpha TH, \\ \dfrac{d}{dt}I = \alpha TH - (\mu_H + \mu_I)I - \beta I C_a, \\ \dfrac{d}{dt}B = \lambda_B - \mu_B B - \gamma_B BT, \\ \dfrac{d}{dt}B_a = \gamma_B BT - (\mu_B + \mu_B^{d\,\mathrm{apop}})B_a + \delta_B B_a T, \\ \dfrac{d}{dt}C = \lambda_C - \mu_C C - \gamma_C CT, \\ \dfrac{d}{dt}C_a = \gamma_C CT - (\mu_C + \mu_B^{d\,\mathrm{apop}})C_a + \delta_C C_a T. \end{cases} \tag{1}$$

In this model, the apoptosis of the activated immune system cells was introduced through

$$\begin{cases} \mu_B^{d\,\mathrm{apop}} = \begin{cases} \mu_B^d; & \text{for } T > T^c, \\ \infty; & \text{for } T \le T^c, \end{cases} \\ \mu_C^{d\,\mathrm{apop}} = \begin{cases} \mu_C^d; & \text{for } I > I^c, \\ \infty; & \text{for } I \le I^c, \end{cases} \end{cases} \tag{2}$$

where T^c and I^c are sufficiently low values of parasites and infected cells, respectively, to the infection be considered eliminated. Hence, system (1) is valid during the time t when $T > T^c$ and $I > I^c$; and when $T \le T^c$ and $I \le I^c$, apoptosis is

activated and the dynamical system is driven to the elimination of the parasite. In other words, activated immune cells, as well as the number of parasites and infected cells, go to zero ($B_a = C_a = T = I = 0$). In a strong immune response, this kind of definition avoids the reappearance of parasites after assuming very low values, which is a mathematical artifact originated from a continuous modeling.

The model does not take into account explicitly the period of time spent to mount the immune response. The delay between the infection and immune response is left to the non-linear terms of activated cells B_a and B_a. Also, the infection term αTH can be understood as the formation of the complex cell–parasite (1 cell and n parasites). Table 1 presents a summary of variables and parameters of the model. Values of the parameters are also given.

The steady states of the system of Eqs. (1) and the stability analysis of the equilibrium points are presented in the case $T > T^c$ and $I > I^c$.

2.1. *Equilibrium points*

The equilibrium points are designated by $(\bar{T}, \bar{H}, \bar{I}, \bar{B}, \bar{B}_a, \bar{C}, \bar{C}_a)$. One of the steady states of the system (1) is the trivial equilibrium point P^0 with coordinates

$$\left(0, H_0 = \frac{\lambda_H}{\mu_H}, 0, B_0 = \frac{\lambda_B}{\mu_B}, 0, C_0 = \frac{\lambda_C}{\mu_C}, 0\right), \tag{3}$$

which corresponds to the sizes of the host and the immune system cells found in an individual free of *T. cruzi* infection.

Table 1. Summary of the variables and parameters of the model and their values. The unity of $[\bullet]$ is number of $\bullet/vu$, with $[I] = [H], [B_a] = [B]$ and $[C_a] = [C]$. Immune response parameters (last six parameters) are allowed to vary.

Symbols	Definitions	Units	Values
T	Concentration of circulating *T. cruzi*	[T]	—
H (I)	Concentration of susceptible (infected) host cells	[H]	—
B (B_a)	Concentration of B cells (plasma cells)	[B]	—
C (C_a)	Concentration of CD8 T cells (cytotoxic cells)	[C]	—
τ	Number of *T. cruzi* released by infected cell	$[T][H]^{-1}$	20
n	Number of *T. cruzi* penetrating susceptible cell	$[T][H]^{-1}$	1
α	Infection rate	day^{-1}	$3\alpha_0$
λ_H	Host cells replenishing rate	day^{-1}	0,2
λ_B	B cells replenishing rate from bone marrow	day^{-1}	0,8
λ_C	CD8 T cells replenishing rate from timus	day^{-1}	0,8
μ_T	*T. cruzi* mortality rate	day^{-1}	0,06
μ_H (μ_I)	Susceptible cells mortality rate (infected cells)	day^{-1}	0,01 (0.05)
μ_B (μ_B^d)	B cells mortality rate (additional)	day^{-1}	0,05 (0.2)
μ_C (μ_C^d)	CD8 T cells mortality rate (additional)	day^{-1}	0,05 (0.2)
γ_B	B cells activation rate	$[T]^{-1}\text{day}^{-1}$	0,01
γ_C	CD8 T cells activation rate	$[T]^{-1}\text{day}^{-1}$	0,01
δ_B	Plasma cells proliferation rate	$[T]^{-1}\text{day}^{-1}$	0,05
δ_C	Cytotoxic cells proliferation rate	$[T]^{-1}\text{day}^{-1}$	0,05
β	Cellular response rate	$[C]^{-1}\text{day}^{-1}$	0,1
ε	Humoral response rate	$[B]^{-1}\text{day}^{-1}$	0,1

In order to become more concise, for the coordinates of the non-trivial equilibrium point P^*, the following dimensionless parameters are introduced

$$\begin{cases} \alpha' = \dfrac{\alpha}{\mu_H} & \alpha'_0 = \dfrac{\alpha_0}{\mu_H} & \delta'_B = \dfrac{\delta_B}{\mu_B + \mu_B^d} & \delta'_C = \dfrac{\delta_C}{\mu_C + \mu_C^d} \\ \beta' = \dfrac{\beta}{\mu_H + \mu_I} & \varepsilon' = \dfrac{\varepsilon}{\mu_T} & \gamma'_B = \dfrac{\gamma_B}{\mu_B} & \gamma'_C = \dfrac{\gamma_C}{\mu_C} \\ \mu_{HI} = \dfrac{\mu_H}{\mu_H + \mu_I} & \mu_{HT} = \dfrac{\mu_H}{\mu_T} & \mu_{Bd} = \dfrac{\mu_B}{\mu_B + \mu_B^d} & \mu_{Cd} = \dfrac{\mu_C}{\mu_C + \mu_C^d}, \end{cases}$$

where α_0 is the threshold of the infection rate α, defined by

$$\alpha_0 = \frac{\mu_T \mu_H}{(\tau - n)\lambda_H} = \frac{\mu_T}{(\tau - n)H_0}, \tag{4}$$

with H_0 being given by Eq. (3).

The coordinates of the unique non-trivial equilibrium point P^*, under the action of the immune response, are

$$\begin{cases} \bar{H} = \dfrac{H_0}{1 + \alpha'\bar{T}} & \bar{I} = \dfrac{\mu_{HI}\alpha' H_0 \bar{T}}{(1 + \alpha'\bar{T})(1 + \beta'\bar{C}_a)}, \\ \bar{B} = \dfrac{B_0}{1 + \gamma'_B\bar{T}} & \bar{B}_a = \dfrac{\mu_{Bd}\gamma'_B B_0 \bar{T}}{(1 + \gamma'_B\bar{T})(1 - \delta'_B\bar{T})}, \\ \bar{C} = \dfrac{C_0}{1 + \gamma'_C\bar{T}} & \bar{C}_a = \dfrac{\mu_{Cd}\gamma'_C C_0 \bar{T}}{(1 + \gamma'_C\bar{T})(1 - \delta'_C\bar{T})}, \end{cases} \tag{5}$$

where $\bar{T}$ is the positive solution of the equation

$$f(T) = T \times g(T), \tag{6}$$

with the fifth $f(T)$ and the third $g(T)$ degree polynomials being given by

$$\begin{cases} f(T) = \left[\left(\dfrac{\alpha'}{\alpha'_0} - 1\right) - \alpha' T\right](1 - \delta'_B T)(1 - \delta'_C T)(1 + \gamma'_B T)(1 + \gamma'_C T) \\ g(T) = \beta'\gamma'_C C_0(1 - \delta'_B T)(1 + \gamma'_B T)(1 + \alpha' T) + \varepsilon'\gamma'_B B_0(1 - \delta'_C T) \\ \qquad \times (1 + \gamma'_C T)(1 + \alpha' T) + \beta'\varepsilon'\gamma'_C C_0 \gamma'_B B_0(1 + \alpha' T)T \\ \qquad + n\alpha'\beta'\mu_{HT}\gamma'_C C_0 H_0(1 - \delta'_B T)(1 + \gamma'_B T). \end{cases} \tag{7}$$

By inspecting $\bar{B}_a$ and $\bar{C}_a$, the inequalities

$$\bar{T} < T_B = \frac{1}{\delta'_B} = \frac{\mu_B + \mu_B^d}{\delta_B} \quad \text{and} \quad \bar{T} < T_C = \frac{1}{\delta'_C} = \frac{\mu_C + \mu_C^d}{\delta_C} \tag{8}$$

must be satisfied for the equilibrium point to be biologically feasible.

Two special cases are presented. Firstly, in the absence of the immune response ($\gamma'_B = \gamma'_C = 0$), the equilibrium point is

$$\left(\bar{T}_0, \frac{H_0}{1 + \alpha'\bar{T}_0}, \frac{\mu_{HI}\alpha' H_0 \bar{T}_0}{1 + \alpha'\bar{T}_0}, B_0, 0, C_0, 0\right),$$

where H_0, B_0 and C_0 are given by Eq. (3), and the equilibrium value of *T. cruzi* $\bar{T}_0$ is given by

$$\bar{T}_0 = \frac{1}{\alpha'_0} - \frac{1}{\alpha'} = \frac{R_0 - 1}{\alpha'}, \tag{9}$$

which is biologically feasible for $\alpha' > \alpha'_0$ (or $R_0 > 1$), where R_0 is the basic reproduction number of parasites defined by

$$R_0 = \frac{\alpha'}{\alpha'_0} = \frac{\alpha}{\alpha_0} = \frac{\alpha H_0}{\mu_T} \times (\tau - n). \tag{10}$$

This number is interpreted as follows. Suppose that one invading *T. cruzi* infects successfully, during its life span $(1/\mu_T)$, a cell in a completely susceptible population of cells (αH_0). This infected cell releases an average number of τ parasites. However, an average number of n parasites are sequestered to infect another susceptible cell (this penetrating number of parasites must be at least one and much lower than τ, or, $1 \leq n < \tau$). Therefore, R_0 is the average number of viable *T. cruzi* originated from one invading *T. cruzi* in an individual who never had got the infection.

Suppose that the immune system recognizes the invading pathogen ($\gamma'_B > 0$ and $\gamma'_C > 0$), but the activated effector cells do not proliferate. This corresponds to $\delta'_B = \delta'_C = 0$, and the coordinates of this special non-trivial equilibrium P_1^* are such that

$$\begin{cases} \bar{H} = \dfrac{H_0}{1 + \alpha' \bar{T}} & \bar{I} = \dfrac{\mu_{HI} \alpha' H_0 \bar{T}}{(1 + \alpha' \bar{T})(1 + \beta' \bar{C}_a)}, \\ \bar{B} = \dfrac{B_0}{1 + \gamma'_B \bar{T}} & \bar{B}_a = \dfrac{\mu_{Bd} \gamma'_B B_0 \bar{T}}{1 + \gamma'_B \bar{T}}, \\ \bar{C} = \dfrac{C_0}{1 + \gamma'_C \bar{T}} & \bar{C}_a = \dfrac{\mu_{Cd} \gamma'_C C_0 \bar{T}}{1 + \gamma'_C \bar{T}}, \end{cases}$$

where $\bar{T}$ is solution of the equation $f(T) = T \times g(T)$, with $f(T)$ and $g(T)$ being, respectively, the third and the second degree polynomials given by

$$\begin{cases} f(T) = \left[\left(\dfrac{\alpha'}{\alpha'_0} - 1 \right) - \alpha' T \right] (1 + \gamma'_B T)(1 + \gamma'_C T), \\ g(T) = \beta' \gamma'_C C_0 (1 + \gamma'_B T)(1 + \alpha' T) + \varepsilon' \gamma'_B B_0 (1 + \gamma'_C T)(1 + \alpha' T) \\ \qquad + \beta' \varepsilon' \gamma'_C C_0 \gamma'_B B_0 (1 + \alpha' T) T + n \alpha' \beta' \mu_{HT} \gamma'_C C_0 H_0 (1 + \gamma'_B T). \end{cases}$$

It can be shown that $f(T)$ and $g(T)$ have two negative roots, while the third root of $f(T)$, when $\alpha' > \alpha'_0$, is positive, and $f(T) = T \times g(T)$ has a unique positive solution situated in the interval $(0, \chi)$. Notice that, due to the absence of the proliferation, the constraints given in Eq. (8) disappear, resulting in $\chi = \bar{T}_0$, as given by Eq. (9). Hence, it is observed that $0 < \bar{T} < \bar{T}_0$.

In Appendix A, the analysis of Eq. (6) is presented, showing that when $\alpha' > \alpha'_0$, there is a unique positive solution $\bar{T}$, which is situated in the range $(0, \chi)$, where χ

is the minimum among $\bar{T}_0, 1/\delta'_B$ and $1/\delta'_C$, that is,

$$\bar{T} \in (0, \chi), \quad \text{with } \chi = \min\{\bar{T}_0, 1/\delta'_B, 1/\delta'_C\}.$$

Additionally, the positive solution always satisfies the constraints given by Eq. (8).

Summarizing, in the absence of the immune response ($\gamma'_B = \gamma'_C = 0$), the equilibrium point is such that $\bar{T} = \bar{T}_0$ ($\bar{B}_a = 0$ and $\bar{C}_a = 0$), while the activation of immune response without proliferation ($\delta'_B = \delta'_C = 0$) results in P_1^*, with $\bar{T} < \bar{T}_0$. Hence, the recognition of invading *T. cruzi* and the consequent activation of immune cells (expressed by the parameters γ'_B and γ'_C) are essential to initiate the control of the infection. However, the containment of *T. cruzi* infection is achieved effectively by the proliferation of activated immune cells (given by the parameters δ'_B and δ'_C), in which case the equilibrium point is P^*. As proliferation increases (δ'_B or δ'_C increases), the constraint $1/\delta'_B$ or $1/\delta'_C$ decreases even below $\bar{T}_0$, and the level of the circulating *T. cruzi* situates lower than $1/\delta'_B$ or $1/\delta'_C$, that is, $\bar{T} \in (0, \chi)$, with $\chi = \min\{1/\delta'_B, 1/\delta'_C\}$.

2.2. *Stability analysis*

The local stability of the equilibrium points P^0 and P^* given, respectively, by Eqs. (3) and (5) are assessed by linearizing the dynamical system (1) at the equilibria. Results are presented briefly, but detailed analyses of the stability are presented in Appendix B.

The trivial equilibrium point P^0 is locally asymptotically stable for $R_0 < 1$, where the basic reproduction number of parasites R_0 is given by Eq. (10). In this case, it was shown that P^0 is globally stable for $R_0 < 1$.

Depending on the values assigned to the model parameters, the unique nontrivial equilibrium point P^* can be locally asymptotically stable for $R_0 > 1$.

3. Numerical Results

Antibodies produced and excreted by plasma cells that neutralize the circulating parasites and cytotoxic actions of activated CD8 T cells that kill infected cells acting coordinately to control *T. cruzi* infection are analyzed numerically, taking into account the values of the model parameters given in Table 1.[1,12] Values of the immune response parameters are allowed to vary.

Based on the values given in Table 1, the equilibrium value of *T. cruzi* is $\bar{T} = 0.624\,\text{parasite/vu}$, where vu stands for an arbitrary volume unit, and the threshold of the infection rate is $\alpha_0 = 1.579 \times 10^{-4}\,[T]^{-1} \times \text{days}^{-1}$, where $[T] = \text{parasite/vu}$ and the basic reproduction number is $R_0 = 3$. The constraints (upper bounds), using Eq. (8), are $T_B = T_C = 5.0\,\text{parasite/vu}$. Additionally, the trivial equilibrium point P^0 has the natural concentrations $H_0 = 20\,\text{cells/vu}$, $B_0 = 16\,\text{Bcells/vu}$ and $C_0 = 16\,\text{Tcells/vu}$. There are approximately 7000 white blood cells per microliter, hence vu should be $0.005\mu\text{L} = 5\text{nL}$, nanoliter. Hereafter, all units are omitted.

The values of parameters given in Table 1 are fixed in all numerical simulations, except when explicitly cited. These values correspond to a weak immune response, presenting, at non-trivial equilibrium $P^*, \bar{T} = 0.624$, which is 67 times lower than the case without immune response, $\bar{H} = 19.43$ (practically equal to H_0) and $\bar{I} = 5.71 \times 10^{-2}$ (39 times lower than the case without immune response). The immune system cells reach $\bar{B} = \bar{C} = 14.22$ (88.9% of the natural concentrations) and $\bar{B}_a = \bar{C}_a = 0.406$ (2.54% of the natural concentrations).

3.1. *Steady states*

The solution of Eq. (6) is obtained numerically by the bisection method.[13]

Figure 1 shows the unique equilibrium value $\bar{T}$ varying α. Also $\bar{H}, \bar{I}, \bar{B} = \bar{C}$ and $\bar{B}_a = \bar{C}_a$ are shown, which are obtained using Eq. (5). For $\alpha \leq \alpha_0$, the only biologically feasible solution is $\bar{T} = 0$; and for $\alpha > \alpha_0$, besides the zero solution a positive solution $\bar{T}$ appears. Due to the values given in Table 1, the steady state values obey $\bar{B} = \bar{C}$ and $\bar{B}_a = \bar{C}_a$. Instead of α, by varying δ_B or δ_C, the equilibrium value of *T. cruzi* is situated always below the upper limits T_B and T_C, satisfying the constraints in Eq. (8). For instance, for $\delta_B = 10^2$, the equilibrium value is $\bar{T} = 2.496 \times 10^{-3}$, with $T_B = 2.5 \times 10^{-3}$, while for $\delta_B = 10^5, \bar{T} = 2.4997 \times 10^{-6}$, with $T_B = 2.5 \times 10^{-6}$. Hence, a unique non-trivial equilibrium point P^* appears for $\alpha > \alpha_0$, and for a fixed α but varying δ_B or δ_C, the coordinate $\bar{T}$ of P^* situates always below the constraints T_B and T_C.

The non-trivial equilibrium point corresponding to the isolated humoral response is LAS in all range of variations of δ_B, as presented in Appendix B. However, for sufficiently higher values of δ_C, the equilibrium point corresponding to the isolated action of cellular response can be unstable. Figure 2 shows the diagram of

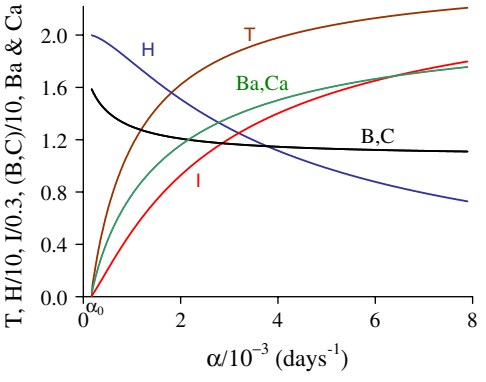

Fig. 1. The equilibrium value of $\bar{T}$, plus all other coordinates of P^*, varying α. The scales of vertical and horizontal axes must be multiplied by the factors shown in the legends to obtain the actual values (for instance, $\bar{H}$ must be multiplied by the factor 10).

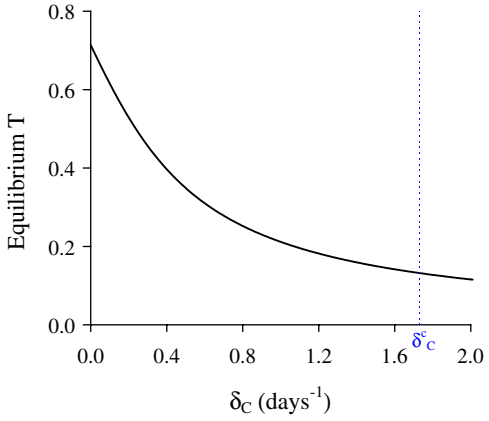

Fig. 2. The diagram of $\bar{T}$ varying δ_C. The equilibrium point P^* is LAS for $\delta_C < \delta_C^c$, and unstable for $\delta_C > \delta_C^c$, where δ_C^c is the critical value.

Table 2. Eigenvalues corresponding to the non-trivial equilibrium P^* obtained using values given in Table 1, except $\delta_C = 1.70$ and $\delta_C = 1.75$.

Eigenvalues	P^* with $\delta_C = 1.70$	P^* with $\delta_C = 1.75$
ψ_1	$-2.45 \times 10^{-1} + i0.0264$	$-2.45 \times 10^{-1} + i0.0260$
ψ_2	$-2.45 \times 10^{-1} - i0.0264$	$-2.45 \times 10^{-1} - i0.0260$
ψ_3	$-2.44 \times 10^{-4} + i0.0821$	$+1.51 \times 10^{-4} + i0.0822$
ψ_4	$-2.44 \times 10^{-4} - i0.0821$	$+1.51 \times 10^{-4} - i0.0822$
ψ_5	-5.12×10^{-2}	-5.12×10^{-2}
ψ_6	-1.01×10^{-2}	-1.01×10^{-2}
ψ_7	-5.13×10^{-2}	-5.13×10^{-2}

$\bar{T}$ varying δ_C, using values given in Table 1. The equilibrium value $\bar{T}$ is LAS for $\delta_C < \delta_C^c$, while for $\delta_C > \delta_C^c$, unstable, where δ_C^c is a critical value.

Table 2 presents the eigenvalues corresponding to the equilibrium P^* calculated with $\delta_C = 1.70$ and 1.75: the first is LAS, while the latter is unstable. By calculating eigenvalues numerically, the interval where the critical value situates is $\delta_C^c \in (1.7305, 1.7310)$: all eigenvalues at the lower bound have negative real part, and at upper bound, a pair of complex numbers has positive real part. A pair of pure complex numbers must be obtained at $\delta_C = \delta_C^c$, and Hopf bifurcation occurs.

3.2. *Evaluating immune responses*

Numerical solutions of Eq. (1) are obtained by the 4th order Runge–Kutta method[13] in order to assess the effect of immune response against *T. cruzi* infection. The initial conditions supplied to the dynamical system (1) are $T(0) = 0.001, H(0) = H_0, I(0) = 0, B(0) = B_0, B_a(0) = 0, C(0) = C_0$ and $C_a(0) = 0$. These conditions simulate *T. cruzi* infection in an individual who had never got this infection.

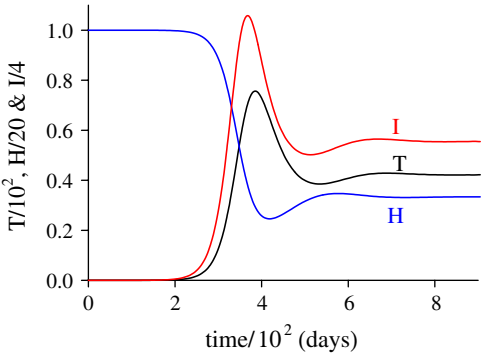

Fig. 3. Dynamical trajectories of *T. cruzi* infection in the absence of immune response. The variables corresponding to immune responses are unchanged (not shown). The scales of vertical and horizontal axes must be multiplied by the factors shown in the legends to obtain the actual values.

Figure 3 shows the case where the immune system does not mount any response, considering $\gamma_B = \gamma_C = 0$. The asymptotic values attained are $\bar{T} = \bar{T}_0 = 2\mu_H/(3\alpha_0) = 42.22$, from Eq. (9) and $\bar{B} = B_0, \bar{C} = C_0$ and $\bar{B}_a = \bar{C}_a = 0$. Other asymptotic values are $\bar{H} = 6.67$ and $\bar{I} = 2.22$.

As shown in Appendix B, the complete elimination of *T. cruzi* is achieved only when $R_0 < 1$, with $R_0 = \alpha H_0(\tau - n)/\mu_T$. Knowing that H_0 is fixed (the number of cells of an organ of human body in general does not vary), *T. cruzi* related parameters α, μ_T, τ and n must be changed in order to reduce R_0. (These parameters can be varied by drug treatments, which are not taken into account.) From a mathematical point of view, the elimination of *T. cruzi* is impossible by the action of immune response alone whenever $R_0 > 1$. Biologically, however, *T. cruzi* can be eliminated if T reaches a very small value (for instance, less than one parasite).

Next, the responses of the immune system in order to reduce *T. cruzi* infection are assessed. For didactical purpose, each one of parameters in the set $(\varepsilon, \gamma_B, \delta_B)$ is varied to assess the strength of the humoral response, while one of $(\beta, \gamma_C, \delta_C)$ is varied to assess the cellular response.

3.2.1. *Enhancing humoral immune response*

The humoral response is described by the destruction of circulating *T. cruzi* by antibodies (ε), the activation of naive B cells (γ_B), and the proliferation of plasma cells (δ_B). Each one of the parameters ε, γ_B and δ_B is increased by 10 and 10^5 times than the value given in Table 1.

Increasing the action of antibodies by 10 times ($\varepsilon = 1$), the dynamical trajectories achieve the asymptotic values $\bar{T} = 0.133, \bar{H} = 19.88$ and $\bar{I} = 8.62 \times 10^{-3}$, while the immune system cells reach $\bar{B} = \bar{C} = 15.59$ and $\bar{B}_a = \bar{C}_a = 8.50 \times 10^{-2}$. This case is similar to weak immune response. Figure 4 shows the increasing action of antibodies by 10^5 times ($\varepsilon = 10^4$), with the asymptotic values reaching

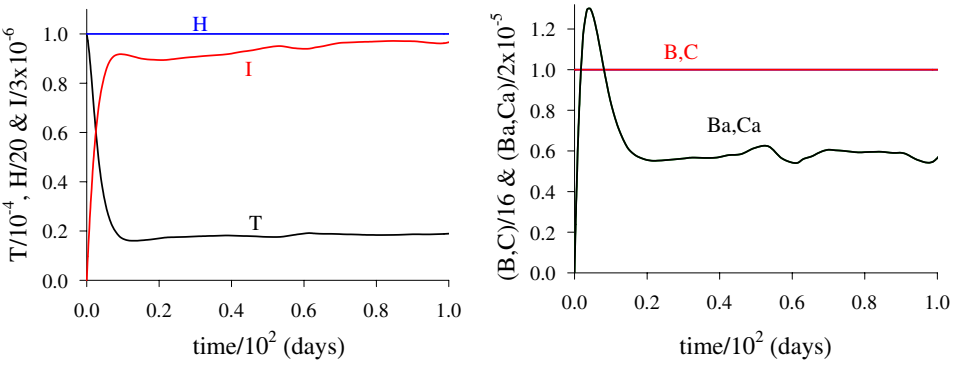

(a) (b)

Fig. 4. Dynamical trajectories of *T. cruzi* infection taking into account the values given in Table 1, except $\varepsilon = 10^4$. The interaction of parasite with host cells T, H and I (a), and the immune response cells B, B_a, C and C_a (b) are shown. The scales of vertical and horizontal axes must be multiplied by the factors shown in the legends to obtain the actual values.

$\bar{T} = 1.87 \times 10^{-5}, \bar{H} = 19.999998$ and $\bar{I} = 2.96 \times 10^{-6}$, shown in Fig. 4(a), and the immune system cells reach $\bar{B} = \bar{C} = 15.99994$ and $\bar{B}_a = \bar{C}_a = 1.20 \times 10^{-5}$, shown in Fig. 4(b). The oscillations are a mathematical artifact, but the asymptotic values are attained.

The increase in ε decreased proportionally the circulating *T. cruzi* ($\bar{T}$) and infected cells ($\bar{I}$). Hence, due to the high affinity and intense production of antibodies, the immune response is enhanced with diminished activation of immune cells, which is the reason for lower numbers of plasma ($\bar{B}_a$) and cytotoxic ($\bar{C}_a$) cells (3×10^4 lower than the weak response).

Increasing the activation of B cells by 10 times ($\gamma_B = 0.1$), the asymptotic values are $\bar{T} = 0.181, \bar{H} = 19.84$ and $\bar{I} = 2.37 \times 10^{-2}$, shown in Fig. 5(a), while the immune system cells reach $\bar{B} = 11.75, \bar{C} = 15.44, \bar{B}_a = 0.88$ and $\bar{C}_a = 0.12$, shown in Fig. 5(b). Increasing the activation by 10^5 times ($\gamma_B = 10^3$), the asymptotic values are $\bar{T} = 2.99 \times 10^{-5}, \bar{H} = 19.99997$ and $\bar{I} = 4.73 \times 10^{-6}$, shown in Fig. 5(c), while the immune system cells reach $\bar{B} = 10.002, \bar{C} = 15.9999, \bar{B}_a = 1.20$ and $\bar{C}_a = 1.92 \times 10^{-5}$, shown in Fig. 5(d).

The increase in γ_B decreased proportionally the circulating *T. cruzi* and infected cells, but slightly less than the action of ε. The high activation of B cells decreased inactivated B cells ($\bar{B}$ in 62.5%), and decreased cytotoxic cells by 10^5 times than plasma cells. In comparison with weak response, $\bar{B}_a$ increased 3 times, while $\bar{C}_a$ decreased 2×10^4 times.

Increasing the proliferation of activated B cells by 10 times ($\delta_B = 0.5$), the equilibrium values are $\bar{T} = 0.345, \bar{H} = 19.69$ and $\bar{I} = 3.92 \times 10^{-2}$, while the immune system cells reach $\bar{B} = \bar{C} = 14.966, \bar{B}_a = 0.67$ and $\bar{C}_a = 0.22$. The dynamical trajectories are similar than those shown in Figs. 5(a) and 5(b), except $B = C$. Figure 6 shows the increasing action of the proliferation by 10^5 times ($\delta_B = 5 \times 10^3$), and the

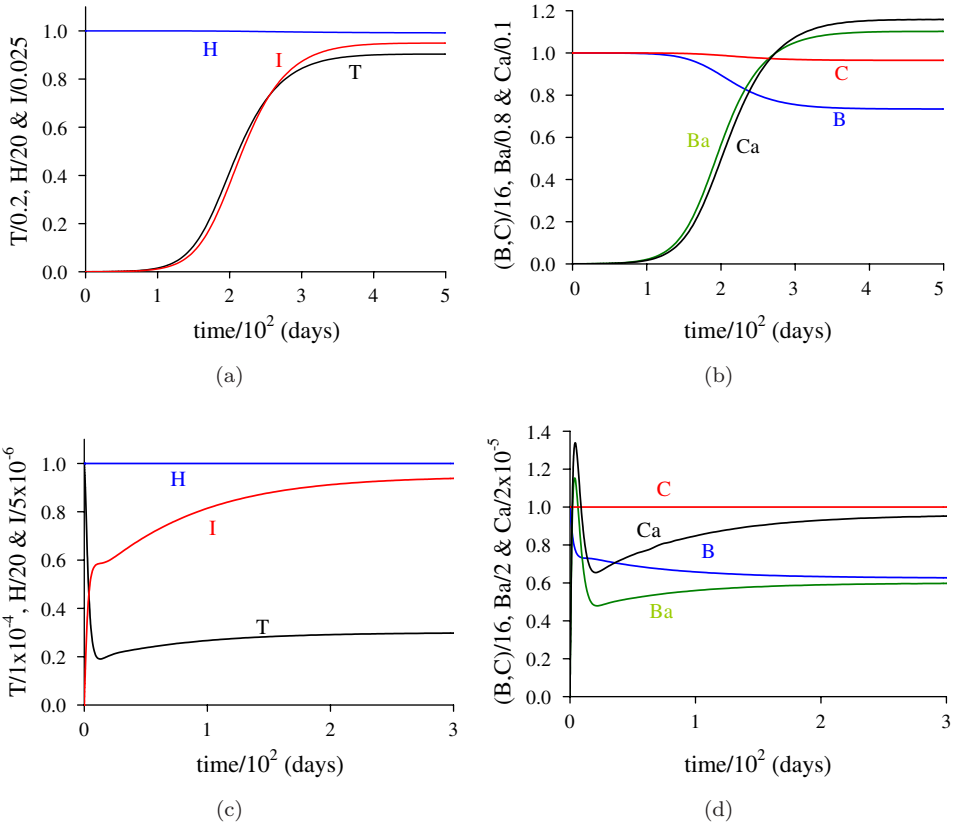

Fig. 5. Dynamical trajectories of *T. cruzi* infection taking into account the values given in Table 1, except γ_B. The interaction of parasite with host cells T, H and I for $\gamma_B = 0.1$ (a) and 10^3 (c), and the immune response cells B, B_a, C and C_a for $\gamma_B = 0.1$ (b) and 10^3 (d) are shown. The scales of vertical and horizontal axes must be multiplied by the factors shown in the legends to obtain the actual values.

asymptotic values are $\bar{T} = 5.00 \times 10^{-5}, \bar{H} = 19.99995$ and $\bar{I} = 7.89 \times 10^{-6}$, shown in Fig. 6(a), while the immune system cells reach $\bar{B} = \bar{C} = 15.9998, \bar{B}_a = 1.20$ and $\bar{C}_a = 3.19 \times 10^{-5}$, shown in Fig. 6(b).

The increase in δ_B decreased proportionally the circulating *T. cruzi* and infected cells, but less than the action of ε. The high proliferation of plasma cells practically unchanged inactivated B cells, but the ratio between plasma cells and cytotoxic cells is quite the same as that observed in the case of activation of B cells.

When one of the parameters ε, γ_B and δ_B is increased by 10^5 times with respect to the value given in Table 1, $\bar{T}$ reached, respectively, $1.87 \times 10^{-5}, 2.99 \times 10^{-5}$ and 5.00×10^{-5}, much less than 6.242×10^{-1} found in weak immune response. The decrease in circulating *T. cruzi* protects host cells from infection, and the infected cells are decreased to, respectively, $2.96 \times 10^{-6}, 4.73 \times 10^{-6}$ and 7.89×10^{-6}, much less than the infection found in the weak immune response, 5.71×10^{-2}. By

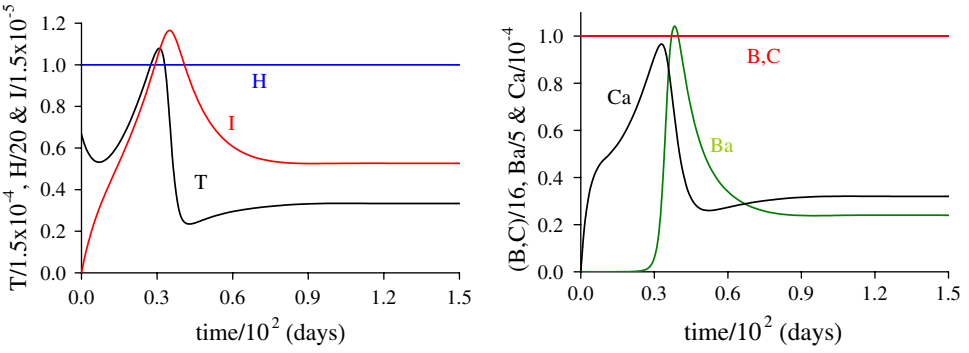

Fig. 6. Dynamical trajectories of *T. cruzi* infection taking into account the values given in Table 1, except $\delta_B = 5 \times 10^3$. The interaction of parasite with host cells T, H and I (a), and the immune response cells B, B_a, C and C_a (b) are shown. The scales of vertical and horizontal axes must be multiplied by the factors shown in the legends to obtain the actual values.

defining arbitrarily $T^c = 1.0 \times 10^{-5}$ and $I^c = 1.0 \times 10^{-6}$ as the values of biological elimination, the increase in one of the humoral response parameters by 10^5 times resulted in a quasi extinction of infection.

Another finding is regarded to the total number of inactivated and activated B and CD8 T cells. The total number of all types of effector cells before the infection is quite the same found after intense immune response.

In all simulations, even if the humoral response parameters are broadly varied (higher than 10^5 times), all dynamical trajectories reach a steady state corresponding to the non-trivial equilibrium point. The model agrees with the simplified model (see Appendix B) with respect to the maintenance of the stability of the non-trivial equilibrium point.

3.2.2. *Enhancing cellular immune response*

The cellular response is described by the destruction of infected cells by *T. cruzi* by action of CD8-positive T cells (β), the activation of naive CD8 T cells (γ_C), and the proliferation of cytotoxic cells (δ_C). The enhanced contribution of cellular immune response against *T. cruzi* infection is studied, by increasing each one of the parameters β, γ_C and δ_C by 10 and 10^5 times than the value given in Table 1, but δ_C is allowed to assume two more values.

Increasing the action of lysis by 10 times ($\beta = 1$), the equilibrium values are $\bar{T} = 0.146, \bar{H} = 19.870$ and $\bar{I} = 1.98 \times 10^{-2}$, while the immune system cells reach $\bar{B} = \bar{C} = 15.55$ and $\bar{B}_a = \bar{C}_a = 9.35 \times 10^{-2}$. Increasing the action of antibodies by 10^5 times ($\beta = 10^4$), the asymptotic values are $\bar{T} = 1.62 \times 10^{-5}, \bar{H} = 19.99998$ and $\bar{I} = 9.37 \times 10^{-7}$, while the immune system cells reach $\bar{B} = \bar{C} = 15.99995$ and $\bar{B}_a = \bar{C}_a = 1.04 \times 10^{-5}$. The dynamical trajectories are similar than those shown in Fig. 4.

The increase in β follows similar behavior with that shown by ε. However, the increase in the capacity of lysis resulted in lower level of circulating *T. cruzi* ($\bar{T}$) and less infection of host cells ($\bar{I}$) than those observed for increasing ε. It shows the importance of cellular defense when parasites invade host cells. The numbers of activated cells are 4×10^4 lower than the weak response.

Increasing the activation of B cells by 10 times ($\gamma_C = 0.1$), the equilibrium values are $\bar{T} = 0.163, \bar{H} = 19.85$ and $\bar{I} = 1.09 \times 10^{-2}$, while the immune system cells reach $\bar{B} = 15.49, \bar{C} = 12.06, \bar{B}_a = 0.10$ and $\bar{C}_a = 0.81$. The dynamical trajectories are similar than those shown in Fig. 5(a) and 5(b), except $B > C$ and $C_a > B_a$. Figure 7 shows the increasing action of the activation by 10^5 times ($\gamma_C = 10^3$), the asymptotic values are $\bar{T} = 2.39 \times 10^{-5}, \bar{H} = 19.99998$ and $\bar{I} = 1.39 \times 10^{-6}$ as shown in Fig. 7(a), while the immune system cells reach $\bar{B} = 15.9999, \bar{C} = 10.818, \bar{B}_a = 1.53 \times 10^{-5}$ and $\bar{C}_a = 1.04$ as shown in Fig. 7(b).

The increase in γ_C follows similar behavior with that shown for γ_B, if the role of B and CD8 T cells is changed. The activation of CD8 T cells resulted in slightly lower levels of *T. cruzi* and infection of host cells. In comparison with weak response, $\bar{C}_a$ increased 2.5 times, while $\bar{B}_a$ decreased 2.3×10^4 times.

When one of the parameters β and γ_C is increased by 10^5 times with respect to the value given in Table 1, $\bar{T}$ reached, respectively, 1.62×10^{-5} and 2.39×10^{-5}, much less than 6.242×10^{-1} found in weak immune response. The decrease in circulating *T. cruzi* protects host cells from infection, and the infected cells are decreased to, respectively, 9.37×10^{-7} and 1.39×10^{-6}, much less than the infection found in weak immune response, 5.71×10^{-2}. In cellular response, the variation in β resulted in $\bar{I} < I^c$ and $\bar{T} \gtrsim T^c$, conditions of a quasi biological elimination of infection. Both $\bar{T}$ and $\bar{I}$ resulted in higher reductions than those observed in humoral response varying ε and γ_B.

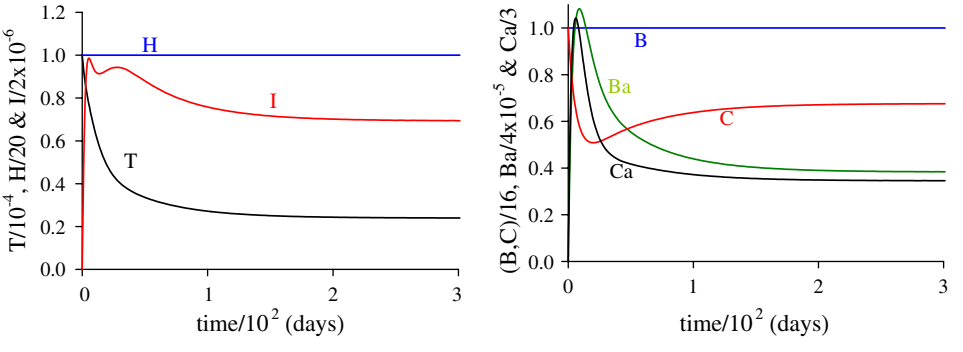

(a) (b)

Fig. 7. Dynamical trajectories of *T. cruzi* infection taking into account the values given in Table 1, except $\gamma_C = 10^3$. The interaction of parasite with host cells T, H and I (a), and the immune response cells B, B_a, C and C_a (b) are shown. The scales of vertical and horizontal axes must be multiplied by the factors shown in the legends to obtain the actual values.

Another finding is regarded to the total number of inactivated and activated B and CD8 T cells. The total number of all types of effector cells before the infection is quite the same found after intense immune response, as it was observed in humoral immune response. In all simulations where β and γ_C are varied broadly, the stability of the non-trivial equilibrium point was unchanged, that is, all dynamical trajectories reach a steady state corresponding to the non-trivial equilibrium point.

The proliferation of activated CD8 T cells is shown in Figs. 8 and 9, for $\delta_C = 0.5, 1.70, 1.75$ and 5×10^3, which are $10, 34, 35$ and 10^5 times greater than the value in Table 1.

Figure 8 shows the case where the non-trivial equilibrium point P^* is stable. For low proliferation rate, $\delta_C = 0.5$, the asymptotic values are $\bar{T} = 0.339, \bar{H} = 19.698$

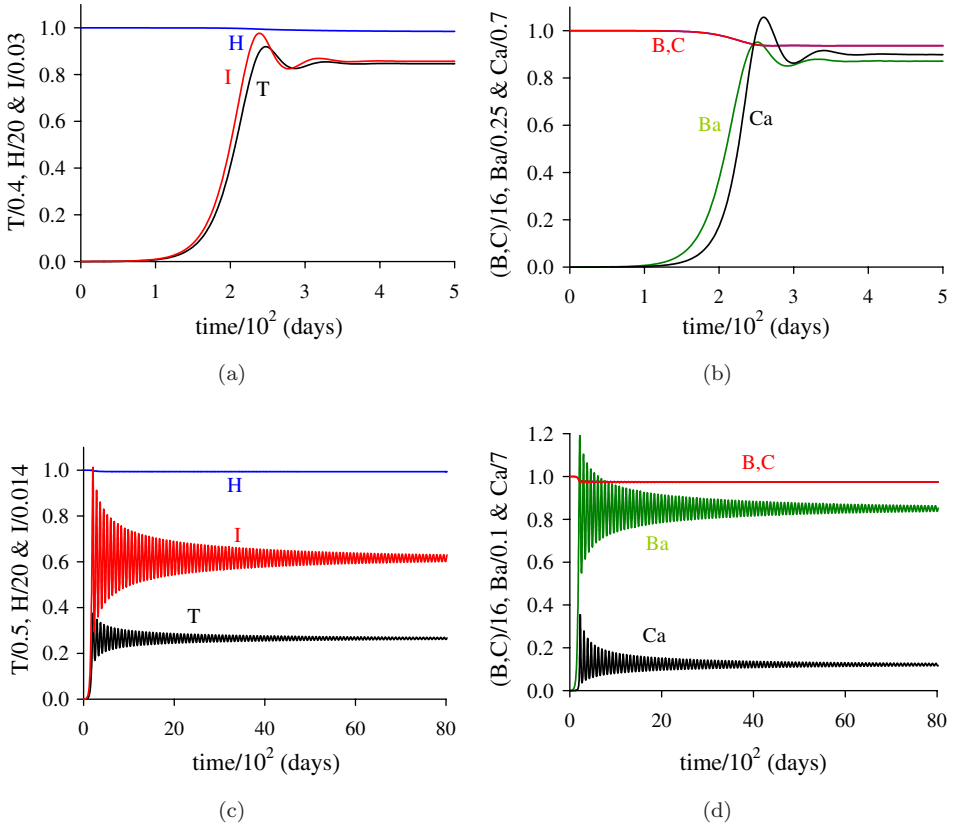

Fig. 8. Dynamical trajectories of *T. cruzi* infection taking into account the values given in Table 1, except δ_C. The interaction of parasite with host cells T, H and I for $\delta_C = 0.5$ (a) and 1.70 (c), and the immune response cells B, B_a, C and C_a for $\delta_C = 0.5$ (b) and 1.70 (d) are shown, which follow damped oscillations. The scales of vertical and horizontal axes must be multiplied by the factors shown in the legends to obtain the actual values.

and $\bar{I} = 2.57 \times 10^{-2}$, shown in Fig. 8(a), while the immune system cells reach $\bar{B} = \bar{C} = 14.985, \bar{B}_a = 0.22$ and $\bar{C}_a = 0.63$, shown in Fig. 8(b). For $\delta_C = 1.70$, the asymptotic values are $\bar{T} = 0.13, \bar{H} = 19.875$ and $\bar{I} = 8.62 \times 10^{-3}$ as shown in Fig. 8(c), while the immune system cells reach $\bar{B} = \bar{C} = 15.586, \bar{B}_a = 8.50 \times 10^{-2}$ and $\bar{C}_a = 0.85$ as shown in Fig. 8(d).

As δ_C increases, but lower than a critical value, the amplitudes of the oscillations increase, as well as the number of oscillations before they fade out. The damped oscillations reach the stable equilibrium point P^*.

Figure 9 shows the case where the non-trivial equilibrium point P^* is unstable and appears a limit cycle. The values corresponding to peak of the variables are also presented. For $\delta_C = 1.75$, the coordinates of unstable equilibrium points are $\bar{T} = 0.13, \bar{H} = 19.88, \bar{I} = 8.38 \times 10^{-3}, \bar{B} = \bar{C} = 15.596, \bar{B}_a = 8.28 \times 10^{-2}$ and $\bar{C}_a = 0.86$. The peaks of variables are $T_p = 0.145, \bar{H} = 19.88$ and $I_p = 9.91 \times 10^{-3}$,

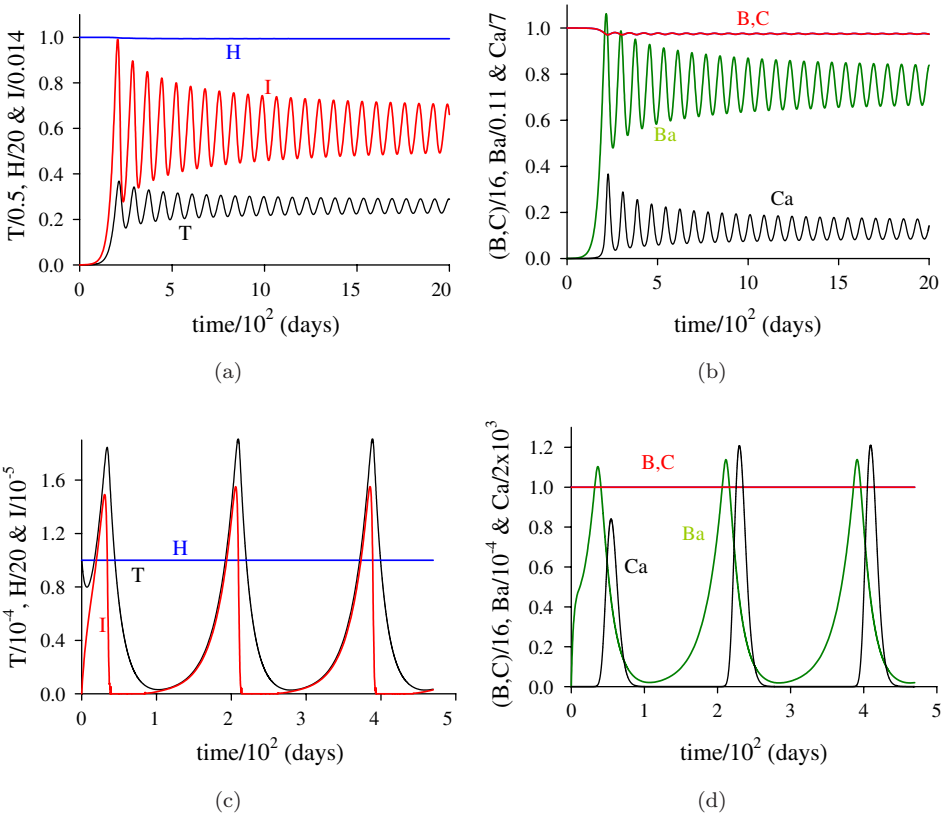

Fig. 9. Dynamical trajectories of *T. cruzi* infection taking into account the values given in Table 1, except δ_C. The interaction of parasite with host cells T, H and I for $\delta_C = 1.75$ (a) and 5×10^3 (c), and the immune response cells B, B_a, C and C_a for $\delta_C = 1.75$ (b) and 5×10^3 (d) are shown, which follow regular oscillations. The scales of vertical and horizontal axes must be multiplied by the factors shown in the legends to obtain the actual values.

shown in Fig. 9(a), while for the immune system cells are $B_p = C_p = 15.62$, $B_{\rm ap} = 9.24\times10^{-2}$ and $C_{\rm ap} = 1.20$, shown in Fig. 9(b). For $\delta_C = 5\times10^3$, the coordinates are $\bar{T} = 4.92\times10^{-5}$, $\bar{H} = 19.99995$, $\bar{I} = 7.75\times10^{-6}$, $\bar{B} = \bar{C} = 15.9998$, $\bar{B}_a = 3.15\times10^{-5}$ and $\bar{C}_a = 2.02\times10^{-3}$. The peaks of variables are $T_p = 1.91\times10^{-4}$, $H_p = 19.99998$ and $I_p = 1.55\times10^{-5}$, shown in Fig. 9(c), while for the immune system cells are $B_p = C_p = 15.99997$ (quasi in equilibrium), $B_{\rm ap} = 1.14\times10^{-4}$ and $C_{\rm ap} = 2.42\times10^3$, shown in Fig. 9(d). Similarly to the action of δ_B, the increase in δ_C decreased the number of plasma cells and increased hugely activated cytotoxic cells.

When δ_C is increased by 10^5 times, the minimum values of T and I reached, respectively, 3.12×10^{-6} and 1.0×10^{-7}. Comparing with previously defined $T^c = 1.0\times10^{-5}$ and $I^c = 1.0\times10^{-6}$ as values of biological elimination, the intense proliferation of activated cytotoxic cells resulted in the extinction of infection according to the biological point of view. Hence, apoptosis must occur elapsing 100 days after the infection, according to Figs. 9(c) and 9(d).

The increase in δ_C resulted in the change of the stability: the non-trivial equilibrium P^* becomes unstable for a critical value of δ_C, say δ_C^c, situated between 1.70 and 1.75. For lower values of δ_C, say $\delta_C \leq 1.70$, the dynamical trajectories follow damped oscillations, while for higher δ_C, say $\delta_C \geq 1.75$, the dynamical trajectories attain limit cycles, and the amplitudes of oscillations of C_a increase with increasing δ_C. For instance, for $\delta_C = 5\times10^3$, the number of effector cells at the peak of dynamical trajectories is about 100 times higher than that found before infection.

Figure 8 shows damped oscillations, while Fig. 9 shows regular oscillations. Table 2 presented the eigenvalues corresponding to Figs. 8(c) and 8(d), with $\delta_C = 1.70$, and Figs. 9(a) and 9(b), with $\delta_C = 1.75$. A pair of pure complex numbers occurred at $\delta_C = \delta_C^c$, where $\delta_C^c \in (1.7305, 1.7310)$. Hence, the numerical results agree with the results of the simplified model (see Appendix B) with respect to the stability of the non-trivial equilibrium point: it becomes unstable for higher values of δ_C, appearing in a limit cycle.

The critical value δ_C^c depends on the values assigned to the parameters. Taking into account the values given in Table 1, if the average number of parasites released by one infected cell is increased by 5 times, $\tau = 100$, it is expected that the critical number decreases, due to increase in the circulating *T. cruzi*. In this case, the critical value situates in the interval $\delta_C^c \in (1.630, 1.635)$. Increasing δ_B by 100 times, or $\delta_B = 5$, which decreases the circulating *T. cruzi*, the critical value is increased, situating in $\delta_C^c \in (5.48, 5.49)$.

4. Discussion

In the foregoing section, it was shown that humoral and cellular immune responses are important in *T. cruzi* infection. The activation of immune cells (parameters γ_B and γ_C) is done by antigen presenting cells (APC), which process and present antigens to immune cells. The simple model presented here did not consider the action of APC neither included the production of cytokines, assuming that the

recruitment (migration) and proliferation of immune response cells were simply proportional to parasite quantity. The activation transfers inactivated (naive, or at rest) to the class of activated cells. In general, small number of cells are activated, which must proliferate quickly and intensively. Numerical simulations showed that as the proliferation (parameters δ_B and δ_C) increases, there is a diminishing of the number of cells being activated from naive cells. However, the intense proliferation results in elevated number of activated cells, which persists even though the parasites were decreased up to biological elimination (described by T^c and I^c). After the containment of parasites the apoptosis must occur in order to decrease rapidly the activated cells. The autonomous model did not take into account the apoptosis. However, this important and crucial question can be introduced in the model by apoptosis described in Eq. (2).

Analysis of the model showed that a well coordinated action of humoral and cellular immune responses is essential to control *T. cruzi* infection. Michailowsky *et al.*,[14] working with the paraflagellar rod proteins (PFR) as a potential vaccine candidate against *T. cruzi* infection, showed that immunization with PFR induced antibodies and protected mice against challenge with a virulent strain of *T. cruzi*. They also demonstrated that protective immunity elicited by vaccination with PFR was dependent on T cells rather than B cells: B-cell-deficient mice immunized with PFR and subsequently challenged with a lethal inoculum of *T. cruzi* presented reduced parasitemia and 100% survival. Immunization with subcutaneous adjuvant as well as PFR with IL-12 simultaneously adsorbed to alum resulted in induction of a Th1 response associated with protective immunity. However, Machado *et al.*,[15] immunizing mice with type 5 recombinant adenoviruses encoding the *T. cruzi* parasite protective antigens trans-sialidase or/and amastigote surface protein-2, showed both optimal antibody and T cell responses and high level of protection against a challenge with live parasites. Further experiments demonstrated that such protection was at least partially dependent on CD8-positive T cells and protection against the *T. cruzi* was highly dependent on type 1 immune response. Since CD8-positive T cells possess effector function to suppress the replication of infectious *T. cruzi* pathogens *in vivo*, the research area aiming for the induction of CD8-positive T cell-mediated protective immunity has become a center of intense research efforts to find control measures against antibody-resistant pathogens.[16]

4.1. *Limit cycle and apoptosis*

For broad ranges of variations of the parameters ε, γ_B and δ_B (humoral) and β and γ_C (cellular), the non-trivial equilibrium point P^* maintained its stability. However, for the parameter δ_C (cellular), the non-trivial equilibrium point P^* always exists for all ranges of its variation, but is stable for lower values only. When δ_C surpasses a critical value δ_C^c, the non-trivial equilibrium point becomes unstable, and limit cycles appear, which can be assessed through the Routh–Hurwitz criteria: δ_C^c is the

value at which one of the criteria is not satisfied firstly. But, this value must be obtained numerically due to the complexity of the coefficients of the seventh degree polynomial. For this reason, the Hopf bifurcation is studied qualitatively.

From Eq. (1) picking up only the equations for T and C_a and rewriting the latter equation, the result is

$$\begin{cases} \dfrac{d}{dt}T = \tau(\mu_H + \mu_I)I - \mu_T T - n\alpha TH - \varepsilon B_a T, \\ \dfrac{d}{dt}C_a = \gamma_C CT - \delta_C(T_C - T)C_a, \end{cases}$$

where T_C is given by Eq. (8). In the equilibrium, $\bar{T} < T_C$ is always obeyed. When δ_C increases, the amount of cytotoxic cells C_a increases, resulting in increasing in the destruction of infected cells I (see Figs. 8 and 9). By decreasing I, lower number of *T. cruzi* T is released, however, B_a is also decreased with increasing δ_C, which decreases the action of antibodies. As a consequence, the first equation for T says that the balance between production and destruction of parasites is such that there is possibility of blow-up in the number of *T. cruzi* for sufficiently higher values of δ_C. This results in $T > T_C$ in the second equation, and C_a increases exponentially, which decreases T, and leads to the decreasing also in C_a. Notice that the upper bound of constraint corresponding to $\delta_C = 5 \times 10^3$ is $T_C = 5 \times 10^{-5}$.

Above qualitatively described limit cycle can be seen in Figs. 9(c) and 9(d). Focusing on the third peak, the increase in both infected cells and parasites begins at around $260\,days$, and reaches peak at around $390\,days$. During this period, T does not surpass T_C, and C_a does not increase. However, just before T reached the peak ($T_p = 19.1 \times 10^{-5}$), T surpassed T_C, and C_a increased exponentially, resulting in a very quick destruction of infected cells I. Due to the fact that the action of antibodies is weak (see Table 1), circulating *T. cruzi* is destroyed slowly, and when it reaches very low value (around $420\,days$) C_a begins exponential decay. This role played between parasites T and cytotoxic cells C_a results in periodic behavior (limit cycle).

Notwithstanding, the limit cycles do not appear with increasing δ_B, even though the governing equations are similar to that for δ_C, that is,

$$\begin{cases} \dfrac{d}{dt}T = \tau(\mu_H + \mu_I)I - \mu_T T - n\alpha TH - \varepsilon B_a T \\ \dfrac{d}{dt}B_a = \gamma_B BT - \delta_B(T_B - T)B_a, \end{cases}$$

where T_B is given by Eq. (8). In this case, T is not allowed to increase as in the previous case, but it always decreases, because with increasing δ_B, increasing B_a and decreasing I are observed (see Fig. 6). From the first equation, the number of released *T. cruzi* by infected cells is decreased, and the action of antibodies is increased by increasing the plasma cells B_a, which decreases T, and T does not

surpass T_B. Hence, T and B_a reach their asymptotic values without oscillations at any point of time.

Efficient immune responses are due to activation (small number of inactivated cells) and subsequent quick proliferation of activated immune cells.[17] Once parasites are cleared, the huge amount of activated cells must be destroyed, mediated by apoptosis. In Fig. 6(b), the equilibrium value $\bar{B}_a$ corresponds to 7.5% of the total amount B_0, while in Fig. 9(d), the peak of C_{ap} corresponds to 15125% of the total amount C_0. Figure 10 illustrates high proliferation of both plasma and cytotoxic cells, letting $\delta_B = \delta_C = 5 \times 10^3$. Figure 10 shows the first two peaks in the beginning of the infection, although regular oscillations (not shown here) are settle after 5000 days. The amplitude of oscillations of C_a is small than the previous case, due to the action of B_a, which decreases T ($T_p = 16.0 \times 10^{-5}$).

From Fig. 10, it is observed that the cytotoxic cells do not blow up (as in Fig. 9), which is due to an intense action of antibodies that are clearing circulating *T. cruzi*. However, the peak of C_{ap} corresponds to 25% of the total amount C_0 (same for plasma cells, due to symmetric values for parameters regarded to humoral and cellular responses). At around 50 days after the infection, T and I drop to minima 7.4×10^{-6} and 6.9×10^{-7}, respectively (B_a and C_a reach the lowest value 3.6×10^{-4} at around 100 days). When T and I drop to minima, *T. cruzi* infection can be considered eliminated (both are lower than T^c and I^c), according to Eq. (2). Hence, at day 50th, apoptosis must occur eliminating all activated cells.

Experiments done with animals[18] showed a little variance of effector cells in comparison with pre-infection values. As shown in Fig. 9, in a very strong cellular immune response, the effector cells after infection are much higher than the level found before, that is, limit cycle implies in a huge amount of immune cells. But,

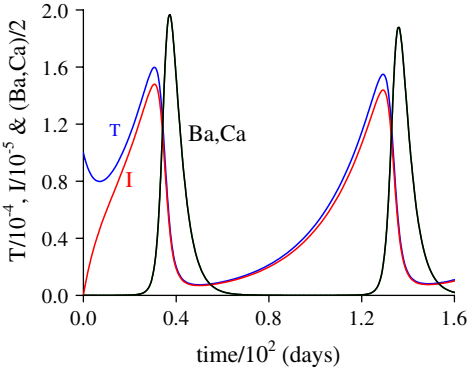

Fig. 10. Dynamical trajectories *T. cruzi* infection taking into account the values given in Table 1, except δ_B and δ_C. The interaction of parasite with host cells (T and I) and the immune response cells (B_a and C_a) for $\delta_B = \delta_C = 5 \times 10^3$ are shown restricting in the beginning of the infection. The scales of vertical and horizontal axes must be multiplied by the factors shown in the legends to obtain the actual values.

as shown in Fig. 10, in a strong humoral immune response, the difference in the number of effector cells before and after infection is little. Comparing Figs. 9 and 10, the limit cycle can be avoided by increasing antibodies related parameters, ε or δ_B, showing that a well orchestrated action of humoral and cellular immune responses is essential to subdue *T. cruzi* infection, and also to avoid sustained oscillations resulting in a relatively small number of activated cells.

4.2. *Parasitemia*

In the early stage of the infection, the transient parasitemia found by El Bouhdidi *et al.*[19] and Andersson *et al.*[20] can be explained by Fig. 11. The initial conditions

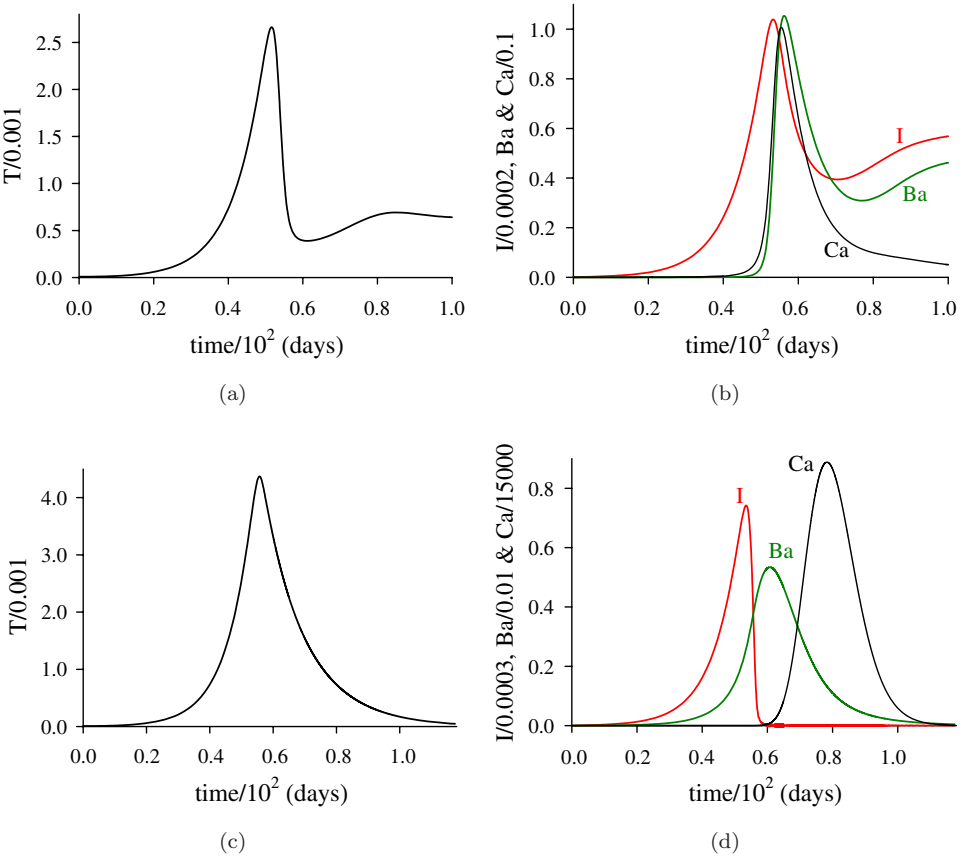

Fig. 11. Dynamical trajectories of *T. cruzi* and infected cells and activated immune response cells taking into account the values given in Table 1, except $\tau = 50, \alpha = 10\alpha_0, \varepsilon = 1, \beta = 1$ and $\delta_C = 300$; and two values for δ_B: $\delta_B = 400$ (a) and (b) and $\delta_B = 50$ (c) and (d). The parasitemia is shown in (a) and (c) and the infected cells and activated immune response cells are shown in (b) and (d). The scales of vertical and horizontal axes must be multiplied by the factors shown in the legends to obtain the actual values.

are the same as those used in previous simulations, except $T(0) = T^c = 0.00001$. The values of parameters are: $\tau = 50$, $\alpha = 10\alpha_0$, $\varepsilon = 1$, $\beta = 1$ and $\delta_C = 300$; and two values for δ_B: $\delta_B = 400$, shown in Figs. 11(a) and 11(b) and $\delta_B = 50$, shown in Figs. 11(c) and 11(d). Other values are those given in Table 1. In Figs. 11(a) and 11(c) the parasitemia is shown, and Figs. 11(b) and 11(d) show the infected and activated immune cells. According to Figs. 11(a) and 11(c), parasitemia lasted up to approximately 8 and 14 weeks, respectively. Higher values of δ_B result in a persistent parasitemia (non-trivial equilibrium point is stable, and from in Fig. 11(a), $\bar{T} = 6.42 \times 10^{-4}$, however the load of parasites in the indeterminate stage can be diminished by increasing δ_B), while for lower values, sustained oscillations are observed (non-trivial equilibrium point is unstable, and in Figs. 11(c) and 11(d) the next peak, not shown here, appears at around 150 days). It is worthy to mention that a decrease in δ_B (decreased proliferation of plasma cells) increased the peak of C_a from 0.1 to 13315.

From Figs. 11(c) and 11(d), the appearance of the first peak occurs in the following order: I, T, B_a and C_a. In a first contact with *T. cruzi* parasite, there is no adaptive immune response, hence, the parasite infects host cells and they grow practically unrestricted. For this reason, the peak of infected host cells firstly appears at around 50 days. Due to abundant parasites, plasma cells produce antibodies, and the maximum production (it is assumed that this production is proportional to the number of B_a) occurs at around 60 days. At this time, parasites begin descending phase, after a peak at around 55 days. Finally, the last peak occurs for C_a at around 80 days. Notice that the infected host cells cannot grow due to the action of cytotoxic cells, and the ascending phase of these cells is roughly proceeded by the end of descending phase of infected cells.

As the infection progresses, the number of parasites in the blood of patients with chronic *T. cruzi* infection is extremely low, and very little is known about the factors that are responsible for parasite persistence and the ensuing chronic disease.[20] The finding of *T. cruzi* in the central vein of suprarenal showed that the presence of the parasites is important in the pathogenesis of the disease, which can be seeded to other sites of the body, especially in immunosuppressed persons.[21] Hence, polymerase chain reaction (PCR) assays have the potential for detecting such low numbers because the organisms have highly repetitive nuclear and kinetoplast DNA sequences that can be amplified by PCR.[1] In a murine model, it was observed that all mice developed a transient parasitemia which lasted up to 8 (infected with the Tulahuen strain) and 12 weeks (infected with the CA-1 clone) post-infection. Another observation was the presence of CD8-positive T cells invading non-necrotic muscle fibers.[20]

The pathogenesis of end-organ destruction in Chagas' disease is not completely understood. The infrequent finding of tissue-dwelling amastigotes in the sectioned heart leads some to argue that amastigotes are sequestered in tissues other than the heart and gut. It is also not clear if continued presence of amastigotes or

parasite DNA is required for tissue destruction. Others believe that infection with *T. cruzi* stimulates auto-immunity, which results in chronic pathological changes in the absence of parasite.[8]

The model considered as the class of host cells H being infected by *T. cruzi* a pool of tissues and organs of human body. Different organs and tissues present broad variability in the risk of infection (α), number of parasites necessary to infect a cell (n) and number of parasites released when an infected cell dies (τ). Each organ or tissue is also characterized by size H_0 of cells. The basic reproduction number of ith organ R_0^i, which is the average number of *T. cruzi* produced by one trypanosome infecting one cell of specified organ, can be defined according to Eq. (10). Highly productive organs and tissues ($R_0^i > 1$) should maintain infection even in a strong immune response,[21] and organs refractory to infection (maybe $R_0^i < 1$), like heart, can eventually sustain *T. cruzi* infection at very lower level. This is left to a further work.

5. Conclusion

Cossy Isasi *et al.*[9] and Sibona *et al.*[10] analyzed mathematical models taking into account the parasite population and action of N different antibodies. The parasites population are released by infected cells, but the dynamics of infected cells do not present healthy cells being infected, rather they increase proportionally to parasites population. Another weakness is the absence of cellular response to kill infected cells.

A simple model presented here dealt with humoral and cellular immune responses against *T. cruzi* infection. Plasma cells (activation described by the parameter γ_B) proliferate (parameter δ_B) and release antibodies that neutralize the protective glycoprotein (parameter ε), exposing the trypomastigotes to complement-mediated lysis. Activated CD8 T cells (activation described by the parameter γ_C) proliferate (parameter δ_C) and produce cytokines, principally IFN-γ capable of activating macrophages to kill intracellular amastigotes (parameter β). The model did not take into account CD4 T helper cells that are necessary to generate both humoral and cellular immune responses. A more elaborate model must consider interleukins or cytokines produced by T helper cells in order to activate and proliferate B and CD8 T cells.

There are evidences of the joint action of humoral and cellular immune responses to control *T. cruzi* infection.[22–27] In experimental murine model of *T. cruzi* infection, a vigorous humoral response accompanied by a significant but moderate TH1 cellular response resulted in control of parasitemia and limited pathology, allowing the recovery and survival of Ninoa-infected mice; in contrast, a weak humoral response with a potent THI proinflammatory profile produced an uncontrolled inflammatory reaction.[27]

An important conclusion from this simple model is the joint action of humoral and immune responses to control *T. cruzi* infection. In general, parasitemia is

contained at a lower but persistent level by immune responses, and the model showed that sustained oscillations occurred when humoral response is less strong than cellular response. This shows the important role played by antibodies in neutralizing circulating trypomastigotes in order to avoid infection of cells. After a strong immune response, effector cells must commit suicide in order to avoid self damage after elimination of parasites.

The model assumed that the class of host cells H is formed by a pool of tissues and organs of human body. If R_0 can be estimated for different organs and tissues, according to Eq. (10), it can be possible to follow the spread of *T. cruzi* infection along different organs and tissues.

The model showed that immune response alone was not able to fade out *T. cruzi* infection, when the reproducibility of this parasite is greater than 1 ($R_0 > 1$). Biologically, however, a critical level of circulating parasites can be defined below which they can be considered eliminated. Hence, there are other types of controls that must be analyzed: administration of chemotherapy and vaccine. The successful elimination of vectorial and transfusional transmission of Chagas' disease in Brazil was a result of the reduction of domestic density of the primary vector *T. infestans* and of almost 100% of coverage in blood serological selection. Thus, the transmission, if it is occurring, is only accidental. However, congenital transmission may occur at any time of pregnancy, in successive gestations and may affect twins. The infection may produce pathology in the growing fetus. The consequences on the newborn are variable, ranging from asymptomatic to severe clinical manifestations. Congenital transmission cannot be prevented, but early diagnosis of the newborn enables prompt treatment, achieving cure rates close to 100% (the treatment regimen should include benznidazol between 5 and 10 mg/kg/d for 30–60 days or nifurtimox at 10–15 mg/kg/d for 60 days) and thus avoiding progression to chronic Chagas' disease.[7] On the other hand, non-antibodymediated cellular immune responses to the antigens expressed in the mammalian forms of the parasite can be used for the purpose of vaccination.[28] In a future work, controlling mechanisms will be included in the model in order to assess the effects of different controls.

Acknowledgments

Project supported through grant from FAPESP – Projeto temático, 2009/15098-0. Thanks to the two anonymous reviewers for providing comments and suggestions, which contributed to improving this paper.

References

1. Mandell GL, Bennett JE, Dolin R, *Mandell, Douglas and Bennett's Principles and Practice of Infectious Diseases*, Elsevier Inc., Philadelphia, 2005.
2. Inaba H, Sekine H, A mathematical model for Chagas disease with infection-age-dependent infectivity, *Math Biosci* **190**:39–69, 2004.

3. Kribs-Zaleta CM, Vector consumption and contact process saturation in sylvatic transmission of Chagas' disease, *Math Popul Stud* **13**(3):135–152, 2006.
4. Cohen JE, Gürtler RE, Modeling household transmission of American trypanosomiasis, *Science* **293**:694–698, 2001.
5. Kleinman SH, Busch MP, The risk of transfusion-transmitted infection: Direct estimation and mathematical modelling, *Baillière's Clin Haematol* **13**(4):631–649, 2000.
6. Slimi R, El Yacoubi S, Dumonteil E, Gourbière S, A cellular automata model for Chagas disease, *Appl Math Model* **33**:1072–1085, 2009.
7. Raimundo SM, Massad E, Yang HM, Modelling congenital transmission of Chagas' disease, *Biosystems* **99**:215–222, 2010.
8. Strickland GT, *Hunter's Tropical Medicine and Emerging Infectious Diseases*, WB Saunders Co., Philadelphia, 2000.
9. Isasi SC, Sibona GJ, Condat CA, A simple model for the interaction between *T. cruzi* and its antibodies during Chagas infection, *J Theor Biol* **208**(1):1–13, 2001.
10. Sibona GJ, Condat CA, Isasi SC, Dynamics of the antibody — *T. cruzi* competition during Chagas infection: Prognostic relevance of intracellular replication, *Phys Rev E* **71**:1–4, 2005.
11. Velasco-Hernandez JX, Perez-Chavela E, A preliminary report on a model for the immune response to *Trypanosoma cruzi*, in Martelli M, Cooke K, Cumberbatch E, Tang B, Thieme H (eds)., *Differential Equations and Applications to Biology and to Industry*, World Scientific, New Jersey, pp. 521–530, 1996.
12. Daniels VG, Wheater PR, Burkitt HG, *Functional Histology*: *A Text and Colour Atlas*, Churchill Livingstone, Edinburgh, 1979.
13. Press WH, Flannery BP, Teukolsky SA, Vetterling WT, *Numerical Recipes. The Arts of Scientifc Computing* (*FORTRAN Version*), Cambridge University Press, Cambridge, 1989.
14. Michailowsky W, Luhrs K, Rocha MOC, Fouts D, Gazzinelli RT, Manning JE, Humoral and cellular immune response to *Trypanosoma cruzi*-derived paraflagellar rod proteins in patients with Chagas' disease, *Infect Immun* **71**(6):3165–3171, 2003.
15. Machado AV, Cardoso JE, Claser C, Rodrigues MM, Grazzinelli RT, Bruna-Romero O, Long-term protective immunity induced against *Trypanosoma cruzi* infection after vaccination with recombinant adenoviruses encoding amastigote surface protein-2 and trans-sialidade, *Hum Gene Ther* **17**:898–908, 2006.
16. Miyahira Y, *Trypanosoma cruzi* infection from the view of $CD8^+$ T cell immunity — An infection model for developing T cell vaccine, *Parasitol Int* **57**:38–48, 2008.
17. Adkinson NF, Yunginger JW, Busse WW, Bocher BS, Holgate ST, Simons FER, *Middleton's Allergy*: *Principles & Practice*, Mosby Inc., Philadelphia, 2003.
18. Thuita JK, Kagira JM, Mwangangi D, Matovu E, Turner CMR, Masiga D, *Trypanosoma brucei rhodesiense* transmitted by a single tsetse fly bite in vervet monkeys as a model of human African trypanosomiasis, *PLoS Negl Trop Dis* **2**(5):e238, 2008.
19. El Bouhdidi A, Truyens C, Rivera MT, Bazin H, Carlier I, *Trypanosoma cruzi* infection in mice induces a polyisotypic hypergammaglobulinaemia and parasite-specific response involving high IgG2a concentrations and highly avid IgG1 antibodies, *Parasite Immunol* **16**:69–76, 1994.
20. Andersson J, Örn A, Sunnemark D, Chronic murine Chagas' disease: The impact of host and parasite genetypes, *Immunol Lett* **86**:207–212, 2003.
21. Castro C, Macêdo V, Prata A, Comportamento da parasitemia pelo *Trypanosoma cruzi* em chagásicos crônicos durante 13 anos, *Rev Soc Brasil Med Trop* **32**(2):157–165, 1999.
22. Sher A, Coffman RL, Regulation of immunity to parasites by T cells and T cell-derived cytokines, *Annu Rev lmmunol* **10**:385–409, 1992.

23. Planelles L, Thomas MC, Alonso C, López MC, DNA immunization with *Trypanosoma cruzi* HSP70 fused to the KMP11 protein elicits a cytotoxic and humoral immune response against the antigen and leads to protection, *Infect Immun* **69**(1):6558–6563, 2001.
24. Garg N, Tarleton RL, Genetic immunization elicits antigen-specific protective immune responses and decreases disease severity in *Trypanosoma cruzi* infection, *Infect Immun* **70**(10):5547–5555, 2002.
25. Pereira VRA, Lorena VMB, Nakazawa M, Luna CF, Silva ED, Ferreira AGP, Krieger MA, Goldenberg S, Soares MBP, Coutinho EM, Correa-Oliveira R, Gomes YM, Humoral and cellular immune responses in BALB/c and C57BL/6 mice immunized with cytoplasmic (CRA) and flagellar (FRA) recombinant repetitive antigens, in acute experimental *Trypanosoma cruzi* infection, *Parasitol Res* **96**:154–161, 2005.
26. Martin DL, Weatherly DB, Laucella SA, Cabinian MA, Crim MT, Sullivan S, Heiges M, Craven SH, Rosenberg CS, Collins MH, Sette A, Postan M, Tarleton RL, $CD8^+$ T-cell responses to *Trypanosoma cruzi* are highly focused on strain-variant trans-sialidase epitopes, *PLoS Pathog* **2**(8):e77, 2006.
27. Espinoza B, Rico T, Sosa S, Oaxaca E, Vizcaino-Castillo A, Caballero ML, Martínez I, Mexican *Trypanosoma cruzi* TCI strains with different degrees of virulence induce diverse humoral and cellular immune responses in a murine experimental infection model, *J Biomed Biotechnol* **2010**:ID 890672, 2010.
28. Rodrigues MM, Oliveira AC, Bellio M, The immune response to *Trypanosoma cruzi*: Role of toll-like receptors and perspectives for vaccine development, *J Parasitol Res* **2012**:1–12, 2012.
29. Murray JD, *Mathematical Biology*, Springer-Verlag, New York, 1989.
30. Hale JK, *Ordinary Differential Equations*, John Wiley and Sons, New York, 1969.
31. Oliveira LS, Modelando a Interação entre o Sistema Imunológico e o *Trypanosoma cruzi*, Dissertation (port.) Unicamp-Imecc, Campinas, 2010.
32. May RM, *Stability and Complexity in Model Ecosystems*, Princeton University Press, Princeton and Oxford, 2001.

Appendix A. Non-trivial Equilibrium Point

The non-trivial equilibrium value of *T. cruzi* corresponding to model (1), $\bar{T}$, is the positive solution of Eq. (6). Initially, properties of the polynomials $f(T)$ and $g(T)$ are analyzed.

The continuous third degree polynomial $g(T)$, given by Eq. (7), is such that $g(-\infty) = \infty, g(0) = \beta'\gamma'_C C_0 + \varepsilon'\gamma'_B B_0 + n\alpha'\beta'\mu_{HT}\gamma'_C C_0 H_0 > 0$ and $g(\infty) = -\infty$. Hence, $g(T)$ has: (1) zero or two real roots in the interval $(-\infty, 0)$ and (2) one or three real roots in the interval $(0, +\infty)$.

To evaluate the roots of the equation $g(T) = 0$, this is written as $g_1(T) = g_2(T)$, where

$$\begin{cases} g_1(T) = \beta'\gamma'_C C_0(1-\delta'_B T)(1+\gamma'_B T) + \varepsilon'\gamma'_B B_0(1-\delta'_C T)(1+\gamma'_C T) \\ \qquad\qquad + \beta'\varepsilon'\gamma'_C C_0\gamma'_B B_0 T, \\ \\ g_2(T) = -\dfrac{n\alpha'\beta'\mu_{HT}\gamma'_C C_0 H_0(1-\delta'_B T)(1+\gamma'_B T)}{1+\alpha' T}. \end{cases}$$

The second-order polynomial function $g_1(T)$ has one positive root, say T_1^+. Hence, in the interval $(0, T_1^+)$, $g_1(T)$ is positive, and assumes negative values thereafter. The function $g_2(T)$ is such that there is one positive ($T_2^+ = 1/\delta'_B$) and one negative ($-1/\gamma'_B$) roots, and $g_2(T)$ has an asymptote at $T = -1/\alpha'$. There are two possibilities for the graph of $g_2(T)$: (1) For $-1/\alpha' > -1/\gamma'_B, g_2(T)$ is a monotonically increasing function for $T > -1/\alpha'$ with positive root at $T_2^+ = 1/\delta'_B$; (2) if $-1/\alpha' < -1/\gamma'_B, g_2(T)$ is an upward concavity function for $T > -1/\alpha'$ with positive root at $T_2^+ = 1/\delta'_B$. In both cases, $g_2(T)$ is negative in the interval $(0, T_2^+)$ and assumes positive values thereafter.

By comparing the behaviors of functions $g_1(T)$ and $g_2(T)$, there is a unique positive root for the equation $g(T) = 0$, say T_g, which is situated between $1/\delta'_B$ and T_1^+: $T_1^+ < T_g < 1/\delta'_B$ (if $g_1(T)$ and $g_2(T)$ intersect at negative value) or $1/\delta'_B < T_g < T_1^+$ (if $g_1(T)$ and $g_2(T)$ intersect at positive value). Hence, $g(T)$ is positive and decreases from $g_2(0)$ up to 0 at $T = T_g$. In turn, the function $T \times g(T)$ is positive in the interval $[0, T_g]$, assuming zero value at the lower and upper bounds of the interval, and has downward concavity.

The continuous fifth degree polynomial $f(T)$, given by Eq. (7), has two negative real roots ($-1/\gamma'_B$ and $-1/\gamma'_C$), two positive real roots ($T_3^+ = 1/\delta'_B$ and $T_4^+ = 1/\delta'_C$) and the last one should be positive or negative. Moreover, $f(-\infty) = \infty, f(0) = R_0 - 1$ and $f(\infty) = -\infty$, where R_0 is given by Eq. (10). When $R_0 > 1$, the last root is positive, $T_5^+ = \bar{T}_0 = f(0)/\alpha'$, with $\bar{T}_0$ being given by Eq. (9). In this situation, $f(T)$ is positive and decreases from $f(0)$ to 0 at $T = \chi$, where χ is the minimum among $\bar{T}_0, 1/\delta'_B$ and $1/\delta'_C$ or $\chi = \min\{\bar{T}_0, 1/\delta'_B, 1/\delta'_C\}$. However, if $R_0 < 1$, the last root is negative, and $f(T)$ is negative and increases from $f(0)$ to 0 at $T = \chi$, where $\chi = \min\{1/\delta'_B, 1/\delta'_C\}$.

The relative positions of the positive roots of $f(T)$, $g_1(T)$ and $g(T)$ are such that: (1) for $\delta'_C > \delta'_B$ (with $g_1(1/\delta'_C) > 0$), $1/\delta'_C < T_1^+ < T_g < 1/\delta'_B$, if $\beta' < \beta'^c$, otherwise, $1/\delta'_C < 1/\delta'_B < T_g < T_1^+$; and (2) for $\delta'_C < \delta'_B$ (with $g_1(1/\delta'_B) > 0$), $1/\delta'_B < T_g < T_1^+ < 1/\delta'_C$, if $\varepsilon' < \varepsilon'^c$, otherwise, there are two possibilities: $1/\delta'_B < T_g < 1/\delta'_C < T_1^+$ or $1/\delta'_B < 1/\delta'_C < T_g < T_1^+$. The critical values $\alpha'^c_B, \alpha'^c_B, \beta'^c$ and ε'^c are

$$\begin{cases} \alpha'^c_B = \dfrac{\alpha'_0 \delta'_B}{\delta'_B - \alpha'_0}, & \beta'^c = \dfrac{(\delta'_C - \delta'_B)(\delta'_B + \gamma'_C)}{\delta'_B \gamma'_C C_0}, \\ \alpha'^c_C = \dfrac{\alpha'_0 \delta'_C}{\delta'_C - \alpha'_0}, & \varepsilon'^c = \dfrac{(\delta'_B - \delta'_C)(\delta'_C + \gamma'_B)}{\delta'_C \gamma'_B B_0}. \end{cases}$$

When $R_0 < 1, T \times g(T)$ is a positive function in the interval $(0, T_g)$ and negative for $T > T_g$, while $f(T)$ assumes negative values in the interval $(0, \chi)$, where $\chi = \min\{1/\delta'_B, 1/\delta'_C\}$, and positive for $T > \chi$ (indeed $f(T)$ assumes again negative values for $T > \max\{1/\delta'_B, 1/\delta'_C\}$, the maximum between $1/\delta'_B$ and $1/\delta'_C$). By the fact that T_g is always greater than $1/\delta'_B$ or $1/\delta'_C$ or both, the curves $y = T \times g(T)$

and $y = f(T)$ intercept at $T > \chi$, which is positive solution but does not obey Eq. (8), resulting in a biologically unfeasible equilibrium. Hence, when $R_0 < 1$, there is not an acceptable positive solution for Eq. (6).

However, for $R_0 > 1$, the function $T \times g(T)$ initially increases from 0 at $T = 0$, and then decreases to 0 at $T = T_g$. But, $f(T)$ decreases monotonically from $f(0) > 0$ at $T = 0$ to 0 at $T = \chi$, where $\chi = \min\{\bar{T}_0, 1/\delta'_B, 1/\delta'_C\}$. Then, the curves $y = T \times g(T)$ and $y = f(T)$ have exactly one intercept in this interval. Hence, $f(T) = T \times g(T)$, Eq. (6), has a unique positive solution $\bar{T}$ in the interval $(0, \chi)$.

Proliferation of plasma and cytotoxic cells affects the magnitude of the unique positive solution $\bar{T}$. This magnitude can be determined, as α' increases, in terms of the critical values $\alpha'^c_B, \alpha'^c_B, \beta'^c$ and ε'^c. Notice that $\alpha'^c_B > \alpha'^c_B$, if $\delta'_B > \delta'_C$, while $\alpha'^c_B < \alpha'^c_B$, if $\delta'_B > \alpha'_0$ and $\delta'_C > \alpha'_0$.

Let the case where plasma cells proliferate higher than cytotoxic cells ($\delta'_B > \delta'_C$) be considered. For $\alpha'_0 < \delta'_C < \delta'_B$, when $\alpha'_0 < \alpha' < \alpha'^c_B$, then $\bar{T} < \bar{T}_0$; when $\alpha'^c_B < \alpha' < \alpha'^c_C$, then $\bar{T} < 1/\delta'_B$; and when $\alpha' > \alpha'^c_C$, then $\bar{T} < 1/\delta'_B$. For $\delta'_C < \alpha'_0 < \delta'_B$, when $\alpha'_0 < \alpha' < \alpha'^c_B$, then $\bar{T} < \bar{T}_0$; and when $\alpha' > \alpha'^c_B$, then $\bar{T} < 1/\delta'_B$. Finally, for $\delta'_C < \delta'_B < \alpha'_0$, $\bar{T} < \bar{T}_0$.

In this case, the concentration of *T. cruzi* at equilibrium $\bar{T}$ situates in the interval $(0, \chi)$, where $\chi = \min\{\bar{T}_0, 1/\delta'_B\}$.

The case corresponding to cytotoxic cells proliferating higher than plasma cells ($\delta'_C > \delta'_B$) is considered. For $\alpha'_0 < \delta'_B < \delta'_C$, when $\alpha'_0 < \alpha' < \alpha'^c_C$, then $\bar{T} < \bar{T}_0$; when $\alpha'^c_C < \alpha' < \alpha'^c_B$, then $\bar{T} < 1/\delta'_C$; and when $\alpha' > \alpha'^c_B$, then $\bar{T} < 1/\delta'_C$. For $\delta'_B < \alpha'_0 < \delta'_C$, when $\alpha'_0 < \alpha' < \alpha'^c_C$, then $\bar{T} < \bar{T}_0$; and when $\alpha' > \alpha'^c_C$, then $\bar{T} < 1/\delta'_C$. Finally, for $\delta'_B < \delta'_C < \alpha'_0$, then $\bar{T} < \bar{T}_0$.

In this case, the concentration of *T. cruzi* at equilibrium $\bar{T}$ situates in the interval $(0, \chi)$, where $\chi = \min\{\bar{T}_0, 1/\delta'_C\}$.

Appendix B. Stability of the Equilibrium Points

The local stability of the equilibrium points is determined by the eigenvalues of the characteristic equation $\det(J^* - \psi I) = 0$, with the Jacobian matrix J being given by $J = [J_1\ J_2]$, where J_1 and J_2 containing, respectively, the first four columns and the last three columns of the matrix J are given by

$$J_1 = \begin{bmatrix} -\mu_T - \varepsilon B_a - n\alpha H & -n\alpha T & \tau(\mu_H + \mu_I) & 0 \\ -\alpha H & -\mu_H - \alpha T & 0 & 0 \\ \alpha H & \alpha T & -\mu_H - \mu_I - \beta C_a & 0 \\ -\gamma_B B & 0 & 0 & -\mu_B - \gamma_B T \\ \gamma_B B + \delta_B B_a & 0 & 0 & \gamma_B T \\ -\gamma_C C & 0 & 0 & 0 \\ \gamma_C C + \delta_C C_a & 0 & 0 & 0 \end{bmatrix}$$

and

$$J_2 = \begin{bmatrix} -\varepsilon T & 0 & 0 \\ 0 & 0 & 0 \\ 0 & 0 & -\beta I \\ 0 & 0 & 0 \\ -(\mu_B + \mu_B^d) + \delta_B T & 0 & 0 \\ 0 & -\mu_C - \gamma_C T & 0 \\ 0 & \gamma_C T & -(\mu_C + \mu_C^d) + \delta_C T \end{bmatrix}.$$

Matrix J^* is the Jacobian J evaluated at the equilibrium point.

B.1. *Trivial equilibrium point*

The eigenvalues corresponding to the trivial equilibrium point P^0, with coordinates given by Eq. (3), are $\psi_1 = -\mu_H, \psi_2 = -\mu_C, \psi_3 = -(\mu_C + \mu_C^d), \psi_4 = -\mu_B, \psi_5 = -(\mu_B + \mu_B^d)$ and the remaining two are the roots of the equation

$$\psi^2 + (\mu_H + \mu_I + \mu_T + n\alpha H_0)\psi + (1 - R_0) = 0,$$

where R_0 is given by Eq. (10). When the coefficients of this second degree polynomial are positive, according to the Routh–Hurwitz criteria,[29] both roots have negative real values, or negative real part if complex. Hence, the trivial equilibrium P^0 is locally asymptotically stable (LAS) if $R_0 < 1$.

To show the global stability of the trivial equilibrium P^0, a Lyapunov function is defined in $V : R_+^7 \to R$ as

$$V = \tau I + T, \tag{B.1}$$

whose orbital derivative is

$$\dot{V} = -\left[\mu_T \left(1 - R_0 \frac{H}{H_0}\right) T + \tau\beta I C_a + \varepsilon B_a T\right].$$

The invariant (biologically feasible) region of the system (1) is given by

$$\Omega = \{(T, H, I, B, B_a, C, C_a) \in R_+^7 \mid T \geq 0; H \leq H_0; I \geq 0; \\ B \leq B_0; B_a \geq 0; C \leq C_0; C_a \geq 0\},$$

where H_0, B_0 and C_0 are given by Eq. (3). Since $H/H_0 \leq 1, \dot{V} < 0$ for $R_0 < 1$ and $\dot{V} = 0$ for $T = 0$. By inspecting the system of Eqs. (1), the maximum invariant set is the trivial equilibrium point P^0. Hence, by the La-Salle Lyapunov Theorem,[30] P^0 is globally stable for $R_0 < 1$.

B.2. *Non-trivial equilibrium point*

When $R_0 > 1, P^0$ becomes unstable, and there arises a unique P^* as shown in the foregoing section. The stability of P^*, with coordinates given by Eq. (5) and $\bar{T}$ as a positive solution of Eq. (6), is assessed by the characteristic equation

$$h_1(\beta, \varepsilon) + \beta \times h_2 + \varepsilon \times h_3 = 0, \tag{B.2}$$

where the functions $h_1(\beta, \varepsilon), h_2$ and h_3 are given by

$$\begin{cases} h_1(\beta,\varepsilon) = (\mu_C + \mu_C^d - \delta_C\bar{T} + \psi)(\mu_C + \gamma_C\bar{T} + \psi)(\mu_B + \mu_B^d - \delta_B\bar{T} + \psi) \\ \qquad\qquad \times (\mu_B + \gamma_B\bar{T} + \psi)[\alpha\bar{T}(\mu_H + \mu_I + \beta\bar{C}_a + \psi)(\mu_T + \varepsilon\bar{B}_a + \psi) \\ \qquad\qquad + (\psi + \mu_H + \mu_I + \mu_T + \varepsilon\bar{B}_a + \beta\bar{C}_a + n\alpha\bar{H})(\mu_H + \psi)\psi], \\ h_2 = \bar{I}\tau(\mu_H + \mu_I)(\mu_B + \mu_B^d - \delta_B\bar{T} + \psi)(\mu_B + \gamma_B\bar{T} + \psi) \\ \qquad \times (\mu_H + \alpha\bar{T} + \psi)[(\gamma_B\bar{B} + \delta_B\bar{B}_a)(\mu_B + \psi) + \gamma_B\delta_B\bar{B}_a\bar{T}], \\ h_3 = \bar{T}(\mu_C + \mu_C^d - \delta_C\bar{T} + \psi)(\mu_C + \gamma_C\bar{T} + \psi)(\mu_H + \mu_I + \beta\bar{C}_a + \psi) \\ \qquad \times (\mu_H + \alpha\bar{T} + \psi)[(\gamma_C\bar{C} + \delta_C\bar{C}_a)(\gamma_C + \psi) + \gamma_C\delta_C\bar{C}_a\bar{T}]. \end{cases}$$

The equalities $\mu_H + \mu_I + \beta\bar{C}_a = \alpha\bar{T}\bar{H}/\bar{I}$ and $\mu_T + \varepsilon\bar{B}_a + n\alpha\bar{H} = \tau(\mu_H + \mu_I)\bar{I}/\bar{T}$ were used to obtain this characteristic equation, hence it is valid only for $\bar{T} \neq 0$. The characteristic equation presents two terms regarding to isolated action of humoral (εh_3) and cellular (βh_2) responses, and one term that accounts for both responses ($h_1(\beta, \varepsilon)$).

The characteristic Eq. (B.2) can be written in the form of a polynomial $\psi^7 + \sum_{i=1}^{7} a_i\psi^{7-i} = 0$. By the fact that the constraints in Eq. (8), $\mu_B + \mu_B^d > \delta_B\bar{T}$ and $\mu_C + \mu_C^d > \delta_C\bar{T}$, are simultaneously satisfied, the equilibrium point P^*, as well as the special equilibrium P_1^*, have positive coefficients $a_i, i = 1, \ldots, 7$. Therefore, one of the Routh–Hurwitz criteria ($a_i > 0, i = 1, \ldots, 7$) is satisfied,[29] implying that the unique non-trivial equilibrium point can be LAS. Instead of dealing with a seventh degree polynomial, the stability of the non-trivial equilibrium point is assessed considering isolated humoral and cellular immune responses.

B.2.1. *Isolated action of humoral response*

When $\beta = 0$ and $n = 0$, the compartments of infected cells, and cytotoxic cells are decoupled from the dynamics, and the non-trivial equilibrium point is $P^* = (\bar{T}, \bar{H}, \bar{B}, \bar{B}_a)$, with coordinates in dimensionless parameters being given by

$$\left(\bar{T}, \bar{H} = \frac{H_0}{1 + \alpha'\bar{T}}, \bar{B} = \frac{B_0}{1 + \gamma_B'\bar{T}}, \bar{B}_a = \frac{\mu_{Bd}\gamma_B' B_0\bar{T}}{(1 - \delta_B'\bar{T})(1 + \gamma_B'\bar{T})}\right),$$

where $\bar{T}$ is solution of the equation

$$\frac{(\frac{\alpha'}{\alpha_0'} - 1) - \alpha' T}{1 + \alpha' T} = \frac{\varepsilon'\gamma_B' B_0 T}{(1 - \delta_B' T)(1 + \gamma_B' T)}$$

and H_0 and B_0 are given by Eq. (3). With respect to the equation for I, this class is considered at steady state, and $(\mu_H + \mu_I)I$ is substituted by αTH in the equation for T.

The characteristic equation corresponding to Jacobian evaluated at the equilibrium point P^* is

$$0 = \varepsilon\bar{T}(\mu_H + \alpha\bar{T} + \psi)[\gamma_B\bar{B}(\mu_B + \psi) + \delta_B\bar{B}_a(\mu_B + \gamma_B\bar{T} + \psi)][(\mu_H + \psi)\psi + \alpha\bar{T}(\mu_T + \varepsilon\bar{B}_a + \psi)] + (\mu_B + \mu_B^d - \delta_B\bar{T} + \psi)(\mu_B + \gamma_B\bar{T} + \psi). \quad \text{(B.3)}$$

This characteristic equation can be written as a polynomial equation $\psi^4 + \sum_{i=1}^{4} a_i\psi^{4-i} = 0$, where the coefficients a_i are

$$\begin{cases} a_1 = (\mu_H + \alpha\bar{T}) + (\mu_B + \gamma_B\bar{T}) + (\mu_B + \mu_B^d - \delta_B\bar{T}), \\ a_2 = (\mu_B + \mu_B^d - \delta_B\bar{T})[(\mu_H + \alpha\bar{T}) + (\mu_B + \gamma_B\bar{T})] \\ \qquad + (\mu_H + \alpha\bar{T})(\mu_B + \gamma_B\bar{T}) + \alpha\bar{T}(\mu_T + \varepsilon\bar{B}_a) + \varepsilon\bar{T}(\gamma_B\bar{B} + \delta_B\bar{B}_a), \\ a_3 = (\mu_H + \alpha\bar{T})(\mu_B + \gamma_B\bar{T})(\mu_B + \mu_B^d - \delta_B\bar{T}) \\ \qquad + [(\mu_B + \gamma_B\bar{T}) + (\mu_B + \mu_B^d - \delta_B\bar{T})]\alpha\bar{T}(\mu_T + \varepsilon\bar{B}_a) \\ \qquad + \varepsilon\bar{T}(\gamma_B\bar{B} + \delta_B\bar{B}_a)[(\mu_H + \alpha\bar{T}) + \mu_B] + \varepsilon\gamma_B\delta_B\bar{T}^2\bar{B}_a, \\ a_4 = \alpha\bar{T}(\mu_T + \varepsilon\bar{B}_a)(\mu_B + \gamma_B\bar{T})(\mu_B + \mu_B^d - \delta_B\bar{T}) + \varepsilon\bar{T}(\mu_H + \alpha\bar{T}) \\ \qquad \times [\mu_B(\gamma_B\bar{B} + \delta_B\bar{B}_a) + \gamma_B\delta_B\bar{T}\bar{B}_a]. \end{cases}$$

It can be shown (omitted here) that, when $\alpha > \alpha_0$, all the Routh–Hurwitz conditions corresponding to the characteristic equation (B.3) are satisfied, which are $a_1 > 0, a_3 > 0, a_4 > 0$ and $a_1a_2a_3 > a_3^2 + a_1^2a_4$.[31]

B.2.2. *Isolated action of cellular response*

When $\varepsilon = 0$ (and a simplification $\tau \gg n$), the compartments of B cells are decoupled from the dynamics, and the non-trivial equilibrium point is $P^* = (\bar{T}, \bar{H}, \bar{I}, \bar{C}, \bar{C}_a)$, with coordinates (dimensionless parameters)

$$\begin{cases} \bar{H} = \dfrac{H_0}{1 + \alpha'\bar{T}}, \quad \bar{I} = \dfrac{\mu_{HI}\alpha' H_0\bar{T}}{(1 + \alpha'\bar{T})(1 + \beta'\bar{C}_a)}, \\ \bar{C} = \dfrac{C_0}{1 + \gamma_C'\bar{T}}, \quad \bar{C}_a = \dfrac{\mu_{Cd}\gamma_C' C_0\bar{T}}{(1 - \delta_C'\bar{T})(1 + \gamma_C'\bar{T})}, \end{cases}$$

where $\bar{T}$ is solution of the equation

$$\frac{(\frac{\alpha'}{\alpha_0'} - 1) - \alpha' T}{1 + \alpha' T} = \frac{\beta'\gamma_C' C_0 T}{(1 - \delta_C' T)(1 + \gamma_C' T)}$$

and H_0 and C_0 are given by Eq. (3).

The characteristic equation corresponding to Jacobian evaluated at the equilibrium point P^* is

$$\begin{aligned} 0 = {} & (\mu_C + \mu_C^d - \delta_C \bar{T} + \psi)(\mu_C + \gamma_C \bar{T} + \psi)[\alpha \bar{T}(\mu_H + \mu_I + \beta \bar{C}_a + \psi)(\mu_T + \psi) \\ & + (\psi + \mu_H + \mu_I + \mu_T + \beta \bar{C}_a)(\mu_H + \psi)\psi] + \beta \bar{I} \tau (\mu_H + \mu_I)(\mu_H + \alpha \bar{T} + \psi) \\ & \times [(\gamma_C \bar{C} + \delta_C \bar{C}_a)(\gamma_C + \psi) + \gamma_C \delta_C \bar{C}_a \bar{T}]. \end{aligned} \tag{B.4}$$

It can be shown (omitted here) the non-trivial equilibrium P^* is locally asymptotically stable for $\alpha > \alpha_0$, but in a limited range of parameter δ_C. The Routh–Hurwitz conditions corresponding to the characteristic equation (B.4) written as a polynomial equation $\psi^5 + \sum_{i=1}^{5} a_i \psi^{5-i} = 0$ are $a_i > 0$ $(i = 1, \ldots, 5)$, $a_1 a_2 a_3 > a_3^2 + a_1^2 a_4$ and $(a_1 a_4 - a_5)(a_1 a_2 a_3 - a_3^2 - a_1^2 a_4) > a_5(a_1 a_2 - a_3)^2 + a_1 a_5^2$.[32] Note that the latter can be written as $a_3(a_1 a_2 - a_3) > a_1^2 a_4$, and, when all coefficients are positive, then an implicit condition is $a_1 a_2 > a_3$, which is not satisfied for a sufficiently higher values of δ_C.[31] When P^* is unstable, due to the fact that there is no other biologically feasible equilibrium, a limit cycle appears.